Université de Montréal

Back Muscles Activity and Scoliosis in Ataxic and Dystrophic Patients

par
Fawzieh SLEEM

Institut de génie biomédical
Faculté de médecine

Mémoire présenté à la Faculté des études supérieures
en vue de l'obtention du grade de maîtrise sciences appliquées (M.Sc.A.)
en génie biomédical

Décembre, 2013

Université de Montréal
Faculté des études supérieures et postdoctorales

Ce mémoire intitulé :

Back muscles activity and scoliosis in ataxic and dystrophic patients

Présentée par :
Fawzieh SLEEM

a été évaluée par un jury composé des personnes suivantes :

Alain VINET, président-rapporteur
Pierre A. MATHIEU, directeur de recherche
Jean-Louis SCHWARTZ, membre du jury

Abstract

To investigate the role of muscles in the development of adolescent idiopathic scoliosis (AIS), our group was initially interested in Duchenne muscular dystrophy (DMD) diseases where a muscular degeneration often leads to scoliosis. Few years ago the studies with those patients provided interesting results but were obtained only from few patients. To increase that number, the present project was initiated but recruitment of new DMD patients from Marie-Enfant hospital was found impossible. As an alternative, patients with Friedreich's ataxia (FA) were recruited since they also suffer from a muscular deficiency which often induces a scoliosis.

So, 4 FA patients and 4 healthy controls have been chosen to closely match the age, weight and body mass indexes (BMI) of the patients were enrolled in our experiments. As in the previous study, electromyography (EMG) activity of paraspinal muscles were recorded on each side of the spine during three types of contraction at 2 different maximum voluntary contractions (MVC). Moreover, the volume and skinfold thickness of these muscles were determined from ultrasound images (US) in order to facilitate the interpretation of EMG signals recorded on the skin surface.

For the 3 FA right scoliotic patients, EMG activity was most of the time larger on the concave side of the deviation. The opposite was found for the 4^{th} one (P4, left scoliosis, 32°) for whom EMG activity was larger on the convex side; it should however be noted that all his signals were of small amplitude. This was associated to a muscle weakness and a large skinfold thickness (12 mm) vs 7 mm for the 3 others. As for the paraspinal muscle volume, it was present on the convex side of P1, P3 and P4 and on the concave side for P2. As for skinfold thickness over this muscle, it was larger on the concave side for P1 and P2 and the opposite for P3 and P4. At the apex of each curve, the volume and skinfold thickness differences were the largest.

Although the study covers only a small number of FA patients, the presence of larger EMG signals on the concave side of a spinal deformation is similar to pre-scoliotic DMD patients for whom the deformation is in its initial stage. It thus seems that our FA patients with more EMG activity on their concave side could see progression of their spinal deformation in the coming months in spite of their already important Cobb angle.

Keywords: DMD, Friedreich's ataxia, Scoliosis, EMG, Ultrasound, Paraspinal muscles.

Résumé

Pour étudier le rôle des muscles dans le développement de la scoliose idiopathique de l'adolescent (SIA), d'abord notre groupe était intéressé par la myopathie de Duchenne (DMD) où une dégénérescence musculaire conduit souvent à la scoliose. Il y a quelques années, des résultats intéressants étaient obtenus par les études avec ces patients, mais seulement de quelques patients. Pour augmenter ce nombre, le présent projet a été lancé, mais le recrutement de nouveaux patients atteints de DMD a été trouvé impossible dans l'hôpital de Marie-Enfant. Comme alternative, les patients atteints de l'ataxie de Friedriech (AF) ont recruté qui provoque un affaiblissement musculaire menant souvent à une scoliose.

Ainsi, 4 patients AF et 4 jeunes sains asymptomatiques constituant le groupe contrôle ont été recruté dans nos expériences. Comme dans l'étude précédente, les signaux électromyographiques (EMG) des muscles paraspinaux ont été captés lors de 3 types de contraction à deux différentes contractions volontaires maximales. En outre, l'épaisseur du pli cutané et du volume de ces muscles ont été déterminées à partir des images échographiques en vue de faciliter l'interprétation des signaux EMG enregistrés à la surface de la peau.

Pour les 3 patients présentaient une scoliose à droite, une activité EMG a été la plupart du temps plus grande sur le côté concave de la déviation. Le contraire a été trouvé chez le 4^{ième} patient (scoliose à gauche, 32°) chez qui l'activité EMG était plus grande sur le côté convexe. Il est à noter que ses signaux EMG étaient très faibles dû à une faiblesse musculaire et à une épaisseur du pli cutané plus grande (12 mm vs 7 mm) pour les 3 autres. En ce qui concerne le volume des muscles paraspinaux, il était plus grand du côté convexe pour P1, P3 et P4 et du côté concave pour P2. Quant à l'épaisseur du pli cutané au-dessus des paraspinaux, il était plus grand du côté concave pour P1 et P2 et c'était l'inverse pour P3 et P4. Ces différences de volume et d'épaisseur du pli cutané étaient plus grandes au voisinage de l'apex des courbes scoliotiques.

Bien que l'étude ne porte que sur un petit nombre de patients atteints de l'ataxie de Friedreich (AF), la présence de signaux EMG plus grands du côté concave de leur déformation vertébrale est à le semblable de ce que nous avons observé chez les patients DMD chez qui une scoliose débutait, une plus grande activité EMG a été détectée sur le côté concave. Il semble donc que les patients AF ayant une activité EMG plus grande du côté concave, pourraient voir leur déformation progresser au cours des prochains mois malgré le fait que leur angle de Cobb soit déjà important.

Mots-clés: DMD, Ataxie de Friedreich, scoliose, EMG, muscles paraspinaux, images échographiques

Table of Contents

List of Tables

List of Figures

List of Abbreviations

AP: action potential

AIS: adolescent idiopathic scoliosis

BMI: body mass index

CDI: cross-sectional area difference index

CK: creatine kinase

CPU: central processing unit

CSA: cross-sectional area

CSN: central nervous system

CT: computerized tomography

DMD: Duchenne muscular dystrophy

ECG: electrocardiography

EMG: electromyography

ES: erector spinae muscles

FA: Friedreich's ataxia

MN: motor neuron

MU: motor unit

MUAP: motor unit action potential

MVC: maximum voluntary contraction

MVIC: maximum voluntary isometric contraction

NMD: neuromuscular disorder

MRI: magnetic resonance imaging

RMS: root mean square

SEMG: surface electromyography

SENIAM: Surface EMG for non-invasive assessment of muscles

SP: spinous process

STR: skinfold thickness ratio

US: ultrasound

Dedicated to my lovely parents, Nawal& Hasan, my soul mate Ali
and my wonderful kids, for their love, endless support
and encouragement.

Acknowledgement

I would never have been able to finish my thesis without the guidance of my director of research, help from friends, and support from my family.

I would like to express my appreciation to my director of research, Dr. Pierre A. Mathieu, for his valuable guidance, supporting and his contribution throughout this research work. It has been an honour to work with him. I would like to express my great appreciation to Dr. Paul Allard, for giving me the permission for using his lab (Laboratoire du mouvement) at Sainte-Justine Hospital. Special thanks to Dr. Farida Cheriet and Dr. Carl Eric Aubin for providing me with the permission to the use their equipments.

I would like to thank my colleague at EMG lab Nahal Najat, who as a good friend was always willing to help and give her best suggestions. Thanks to Youssef Kanaan, for helping me run the experiments, your assistance was priceless. I also gratefully acknowledge Véronique Desjardins for providing precious technical support throughout this project. Special thanks to Hacéne Chebrek, Philippe Debanné, Christian Bellefleur and Julie Joncas at Sainte-Justine Hospital who have been always helpful and cooperative. Many thanks for all my friends at Université de Montréal for their participation in the experiments. My research would not have been possible without their help.

Finally, I would also like to thank my parents, my brothers and my lovely sister. They were always supporting me and encouraging me with their best wishes. My husband, Ali, was always there cheering me up, gave me his unconditional support and love through all this long process. My wonderful kids, Mohamad & Youssef, your existence in my life give me the strength to hang on and never give up.

Chapter 1: Introduction

Scoliosis is a 3D deformation of the spine which mostly affects young girls. When visually detected, the deformation has thus been slowly progressing over a long period. Being practically impossible to identify the factors at the origin of the situation, it is classified as adolescent idiopathic scoliosis (AIS). Fifty-nine percent of all scoliotic patients fit in this category. Many factors such as genetic factors, hormonal imbalance, asymmetric bone growth and muscle imbalance are suspected of participating to such deformations (Machida, 1999). Among those factors, we are interested to the muscular involvement, i.e., an uneven activity of the back muscles which are lying on each side of the spine. To help identify how this factor can lead to the development of scoliosis, our group have already conducted a study on few young Duchenne muscular dystrophy (DMD) patients where it is well known that a muscular deficiency is at the origin of their scoliotic deformation.

DMD disease is associated to a recessive X-chromosome which induces a degeneration of the muscles eventually leading to the loss of ambulation, to scoliosis and to death. First described by the French neurologist Guillaume Duchenne around 1860, DMD is the most common neuromuscular disorders affecting 1 in 4000 males. He attributed the signs and symptoms to a distinct familial disease entity and originally described the condition as a pseudo-hypertrophic muscular paralysis (Bogdanovich et al., 2004). In humans, DMD occurs as a result of mutations (mainly deletions) in the dystrophin gene, located on the Xp21 chromosome. Mutations lead to an absence of, or defect in the protein dystrophin, which induces the progressive muscle degeneration leading to loss of independent ambulation (Ross et al., 2009). Symptoms usually appear at the age about 5 to 6 years, with a general muscle weakness and contractures or stiffness developing in the foot, the knee and the hip joints. The progressive muscle wasting leads, at about 9 to 11 years of age, to the loss of the ability to walk and an electric wheelchair is then used to help the patient to be mobile and have some independence. The use of corticosteroid and respiratory, cardiac, orthopaedic treatments as well as rehabilitative interventions have led to improvements in function, health and a longer life expectancy of DMD children. However no specific therapy is available to cure those patients (Kinali et al., 2008).

With 75–90% of non-ambulatory DMD patients developing scoliosis, muscular weakness is considered to be the factor responsible for the development of the deformation (Bogdanovich et al., 2004). Due to their neuromuscular disorder, DMD patients thus offer a unique situation to study the muscular role in AIS. Knowing in advance that those patients are at great risk of developing scoliosis, it is thus possible to study back muscles activity before, during and following the onset of a scoliosis, an impossible feat with AIS patients.

Muscle activity generates an electrical signal called an electromyogram (EMG). This signal propagates from its source up to the skin surface where it can be detected. Most of the EMG studies with AIS patients have revealed the presence of larger signals on the convex than on the concave side of the deformation, particularly at the apex of the curve (de Oliveira et al., 2011; Cheung et al., 2005; Thouin et al., 2005). Such a difference in paraspinal muscles activity as well as a difference in the stretch receptors activity on the concave as compared to the convex side is considered to play an important role in the development and production of the spinal deformity (Cheung et al., 2005). Since differences in muscle activity between each side of the spine could originate from differences in muscle dimension and muscle wasting (i.e., replacement of muscle fibers by fat and cicatricial tissues), magnetic resonance images (MRI) was used (Zoabli et al., 2008) to analyze ES muscles volume and fatty infiltration factor in scoliotic spine in few DMD patients. It has been shown that the volume of the ES muscle of pre- and scoliotic patients was found smaller on the convex side relative to the concave one. While, the fat infiltration was found larger on the convex side of pre- and scoliotic patients and no significant difference was observed in non-scoliotic patients.

The recruitment of DMD patients in a previous study by our group (Thouin, 2005) was difficult because many research projects are interested with this population. With a more extended use of corticoids which retard their growth spurt and thus reduced the prevalence of scoliosis, their enrollment in our present research protocol was no more possible. We thus decided to work with Freidreich's ataxia (FA) patients who also develop scoliosis due to muscle impairment. FA is a progressive spinal-cerebellar degenerative disorder characterised by a loss of balance and coordination (ataxia). First described by Nikolaus Friedreich in the late 19th century, it affects about one in 50,000 people worldwide, making it the most prevalent inherited ataxia (Pandolfo, 2009; Tsirikos and Smith, 2012). FA pathology results from lack of frataxin which is a

mitochondrial protein important for normal production of cellular energy. A defect in its action may result in abnormal accumulation of iron in mitochondria which results in cellular damage and death. In FA, ataxia results from the degeneration of nerve tissue in the spinal cord and of nerves that control muscle movement in the arms and the legs. The spinal cord becomes thinner and nerve cells lose some of their myelin sheath impairing nerve impulse propagation.

The diagnosis of FA is generally made in mid childhood or early adolescence based upon clinical criteria. For Geoffrey et al. (1976) the primary features consist of onset of symptoms before the age of 20-25 years, progressive ataxia, dysarthria, decreased proprioception and vibratory sense, absent knee and ankle reflexes, muscle weakness, and lack of deep tendon reflexes. Their secondary criteria are cavus foot deformities, scoliosis, cardiomyopathy in up to 90% of patients, optic atrophy and diabetes. The level of function gradually deteriorates with the patients becoming wheelchair-dependent by the second or third decades of life, at which time most patients die due to severe cardiomyopathy (Geoffroy et al., 1976). Later, Harding (1981) proposed less stringent criteria which proved to be very specific but not particularly sensitive (Delatycki and Corben, 2012). No known effective cure or treatment exists for FA. Intervention efforts currently focus on improving symptoms and associated complications in order to help patients in maintaining optimal functions for as long as possible.

As with DMD, nearly all patients with FA (63 to 100%) develop scoliosis (Milbrandt et al., 2008; Cady and Bobechko, 1984). The natural history and treatment of FA scoliosis is limited due to the relative rarity of the condition. Previous reports have described the progression, curve patterns and treatment of the FA scoliosis (Cady and Bobechko, 1984; Labelle et al., 1986; Daher et al., 1985). While some classified it as a neuromuscular scoliosis (Milbrandt et al., 2008) similar to that seen in muscular dystrophy characterized by long C-shaped curves associated with pelvic obliquity and severe muscle weakness, others see it as an idiopathic scoliosis with greater incidences of double major curve patterns, single thoracic and thoracolumbar curves (Labelle et al., 1986).

In the previous project of our group (Thouin, 2005), recruitment of DMD patients at Marie-Enfant hospital proved to be difficult but impossible this time. We thus tried to recruit FA patients but our project did not have a high priority and only 4 scoliotic FA patients were

recruited in spite of a monetary reward of $125. As in the previous study, surface EMG signals on both sides of the spine were recorded on the FA patients and on 4 healthy controls chosen to closely match the age, weight and body mass index (BMI) of the patients. MRI images of the back muscles were used in the Thouin study but access to the scanner was quite restricted. We thus tried to get similar information on back muscles with ultrasound (US) images since the access to such equipment is much easier and studies have already reported the use of US imaging on scoliotic patients (Thaler et al., 2008; Burwell et al., 2002; Kennelly and Stokes, 1993).

In the present study, our objective was thus to study the paraspinal muscles activity along and on each side of the spine of FA patients. To facilitate the interpretation of the collected EMG signals, the volume of those muscles on each side of the spine and their distance from the skin surface was obtained.

Our hypothesis was that similar EMG activity would be displayed by both DMD and FA patients. This implies that an imbalance in back muscle activity induces a larger tension on one side of a spine that induces a bending toward the opposite side. The scoliosis having progressed, a larger EMG activity is frequently observed on the convex side of the deformation. A greater force on the convex side counteracts the deformation and may eventually lead to its disappearance of the scoliosis. The origin of a greater EMG activity on one side of the spine could be associated with a larger muscle volume and/or to a smaller distance between skin surface and superficial paraspinal muscles. It is to assess those factors that ultrasound imaging was used. In absence of any anatomical differences, attention could then be focused on the neural activity which triggers muscle contraction on each side of the spine.

Following this Introduction, the first part of Chapter 2 is used to provide some information on back muscle physiology, on the principles of US imaging, on EMG signals acquisition and processing processed, this is followed by a literature review on DMD, FA and scoliosis. Chapter 3 contains a description of the experimental protocol, of the procedures involved in each experiment with a patient and a short description of the equipment used as well as how it was synchronized for the data collection. Information on how the various data were processed is also presented. In Chapter 4, the results on EMG and on US images analysis are presented. This is

followed by a Discussion of the most interesting results of the project in relation to other published results. In the Conclusion, directions for future research on the role of muscle activity in the development of scoliosis are suggested.

Chapter 2: Literature Review

2.1 Anatomy and Physiology of the Spine

(From Drake et al., 2005 and Agur and Dalley, 2008)

The spine is a combination of 33 rigid bones or vertebrae separated by intervertebral discs. Integrity of that structure is assured by flexible ligaments, inelastic tendons, and many muscles. All of those components are working together to maintain an upright position and assure the mobility required in the accomplishment of various daily life activities (Wattjes et al., 2010).

2.1.1 Elements of the Spine

It is divides in 5 regions: cervical, thoracic, lumbar, sacrum, and coccyx (Fig. 2.1). There are 7 vertebrae in the cervical region, 12 in the thoracic region and 5 in the lumbar region. The other 9 form the sacrum and the coccyx and are fused together which prevent any movement between them. On a lateral view, the spine has an S shape which provides an even distribution of body weight from the head to the feet allowing it to withstand many kinds of stress.

2.1.1.1 Vertebrae

Stacked on top of each other with an in between disc, they are the boney building blocks of the spine. Each vertebra is made of several parts (Fig 2.2): transverse processes are a projection on either side of the vertebral body; the spinous process is the bony portion that can be felt as a series of bumps in the center of a person's neck and back, and the articular processes that are located between the others. All those processes or laminae that are at the back of the vertebral body constitute the spinal canal within which the spinal cord is found. The processes possess facets which act as mechanical stops which limit the movements between the vertebrae and keep maintain their aligned position.

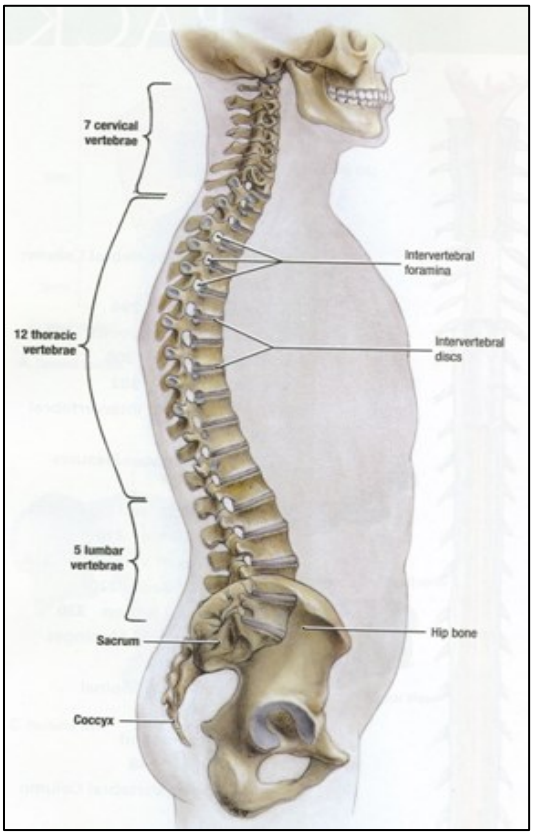

Figure 2.1: Anatomy of the spine (Agur and Dalley, 2008, p.286).

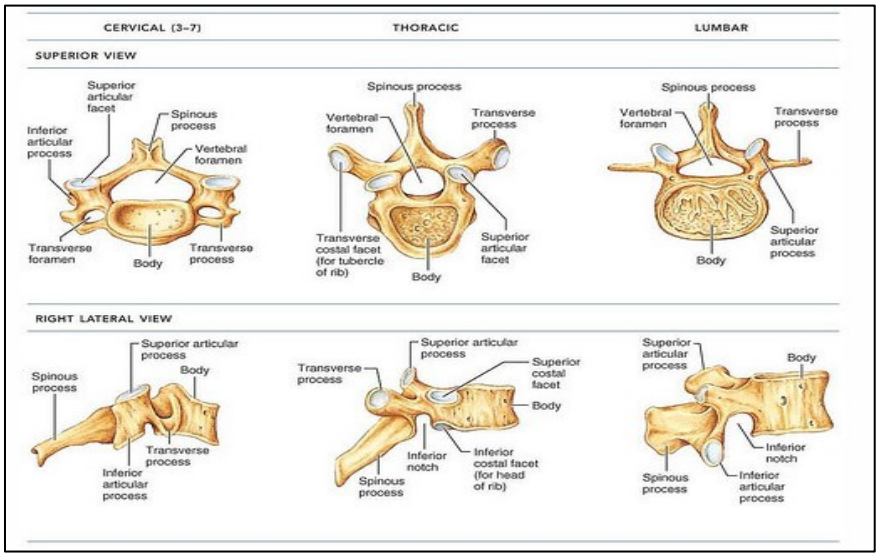

Figure 2.2: Sections of a typical vertebra (Agur and Dalley, 2008, p.289).

2.1.1.2 Intervertebral Disc

These structures are designed to absorb the stresses imposed on the spine while allowing the vertebral bodies to move one relative to its neighbours. Each disc consists of a strong outer ring of fibers called the annulus fibrosis, and a soft center called the nucleus pulposus which is made of a semi-fluid gel (Fig.2.3). The nucleus provides elasticity and compressibility while the annulus fibrosus contains and limits the expansion of the nucleus.

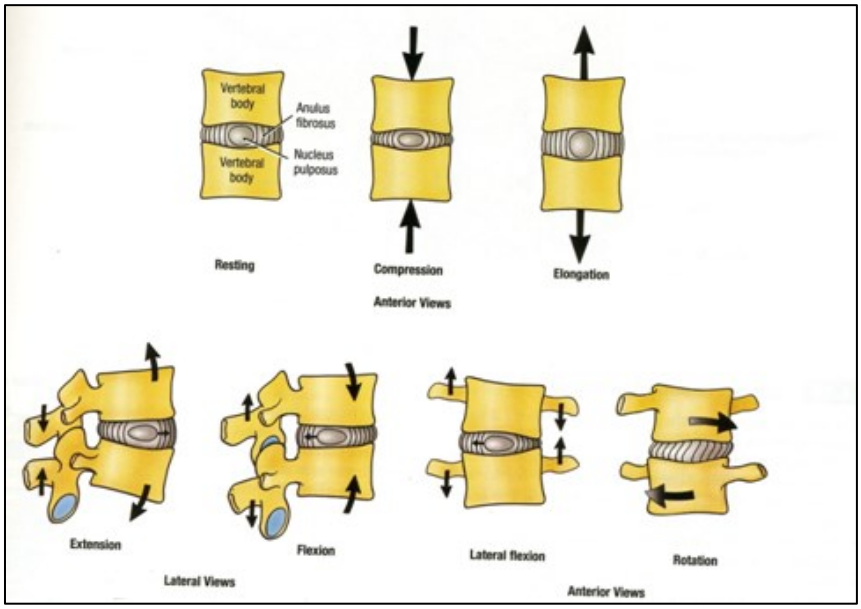

Figure 2.3: Intervertebral disc: ligaments and movements (Agur and Dalley, 2008, p.307).

2.1.1.3 Ligaments

Ligaments are fibrous tissues that connect two or more bones, attach the vertebrae together and thus control the movements between vertebrae. During bone injury, the ligament can aid to its restoration and help maintain stability.

2.1.2 Paraspinal Muscles

The function of back or paraspinal muscles is to stabilize all the vertebrae, influence posture, and extend, flex, and rotate the spinal column. They are organized in layers and the length of their fibers is short for muscle fibers lying in the deepest layer while long ones are more superficial and may be described as a system of guy-ropes. While superficial back muscles are involved in movements of the upper limb, the intermediate layer consist of muscles attached to the ribs and

have a respiratory function. Deep or intrinsic muscles extend from the pelvis to the skull. The erector spinae which forms the most powerful muscle group associated with the spine is located in the intermediate part of the deep layer (Drake et al., 2005).

2.1.2.1 Erector spinae (ES) muscles

The ES runs along each side of the spinal column. Arising from a tendon attached to the crest along the centre of the sacrum (the part of the backbone at the level of the pelvis), it is made up of three muscles: the spinalis located most medially, the longissimus in the center and iliocostalis laterally (Fig. 2.4).

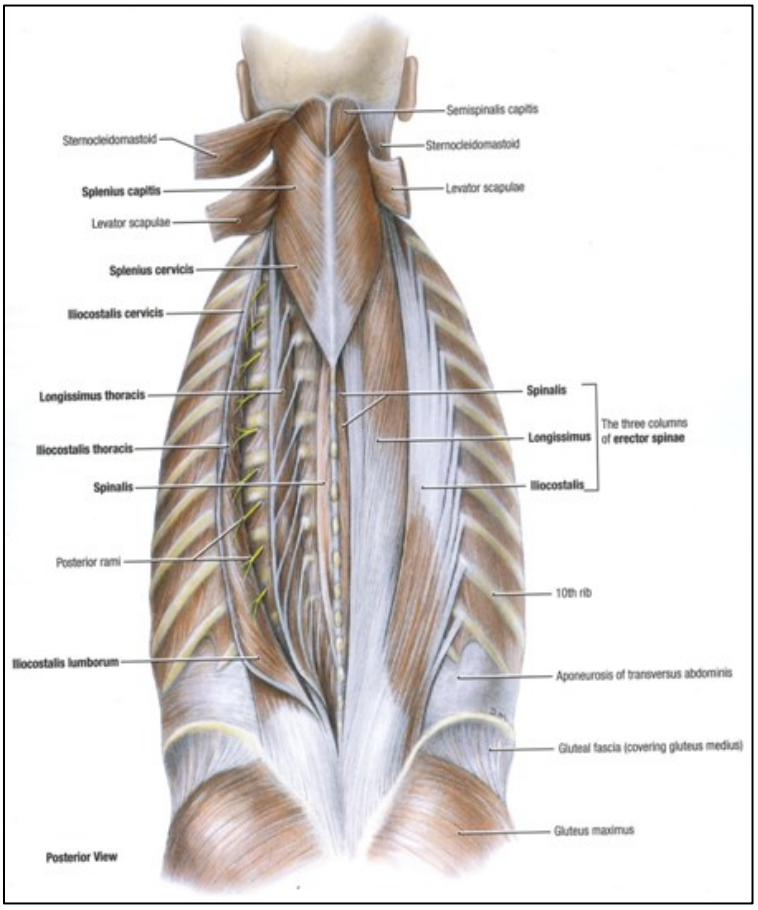

Figure 2.4: The erector spinae group is made up of three muscles: the spinalis most medially, the longissimus in the center, and iliocostalis laterally (Agur and Dalley, 2008, p.323).

The ES muscles are the primary extensors of the vertebral column and head. They straighten the back, returning it to the upright position from a flexed position, and pull the head posteriorly.

They also participate in controlling vertebral column flexion by contracting and relaxing in a coordinate fashion. When unilaterally contracted, they bend the vertebral column to the left or to the right and at the head level, turn it toward the actively contracting side (Drake et al., 2005).

2.2 Cobb angle

It is the standard method used to measure and quantify the magnitude of spinal deformities in scoliosis cases. It is defined, as we can see in Fig 2.5, as the angle formed between a line drawn parallel to the superior endplate of one vertebra above the apex and another one drawn parallel to the inferior endplate of the vertebra below the apex. The angle may be plotted manually or digitally and scoliosis is defined as a lateral spinal curvature with a Cobb angle of 10° or more.

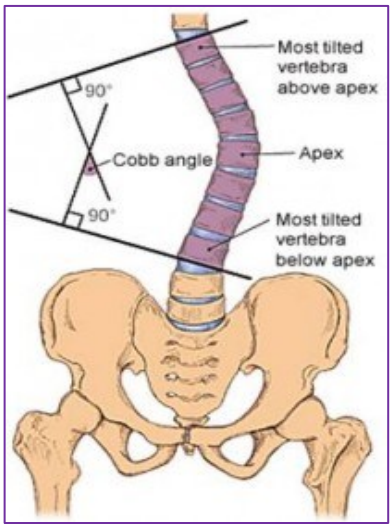

Figure 2.5: Cobb method measurement. Choose the most tilted vertebrae above and below the apex of the curve. The angle between intersecting lines drawn perpendicular to the and lower upper end vertebra is the Cobb angle (from:http://www.tweedcoastchiropractic.com.au/ OurServices/ Chiropractic/Scoliosis.aspx).

2.3 Electromyography (EMG)

Associated with the ionic currents at the origin of a muscle contraction, an electromyographic (EMG) signal can be detected at the skin surface through the use of electrodes (Basmajian and DeLuca, 1985). Analysis of EMG signals is used in many areas of human movement and for neuromuscular diagnostics (Stegeman et al., 2000). As a research tool, it has been used to study

the paraspinal muscles activity in patients with low-back pain symptoms, postural disorders, as well as evaluating muscle imbalance in scoliotic patients (Odermatt et al., 2003, Bassani et al., 2008). EMG recording can be achieved invasively with one or few electrodes inserted in a muscle (intramuscular recordings) or non-invasively with electrodes placed over the skin.

2.3.1 EMG Signal Generation and Detection

2.3.1.1 The Motor Unit

Muscle is composed of excitable muscle fibers which are cells shaped like cylinders which are grouped in bundles. When excited, the intracellular action potential (AP) which propagates all along each fiber induces its contraction. As initially described by Sherrington (1929), muscle fibers are organized in groups called motor units (MUs) made of a motor neuron (MN) and all of the muscle fibers that it innervates (Fig. 2.6). The summation of the signals originating from all activated muscle fibers of a MU is called a motor unit action potential (MUAP).

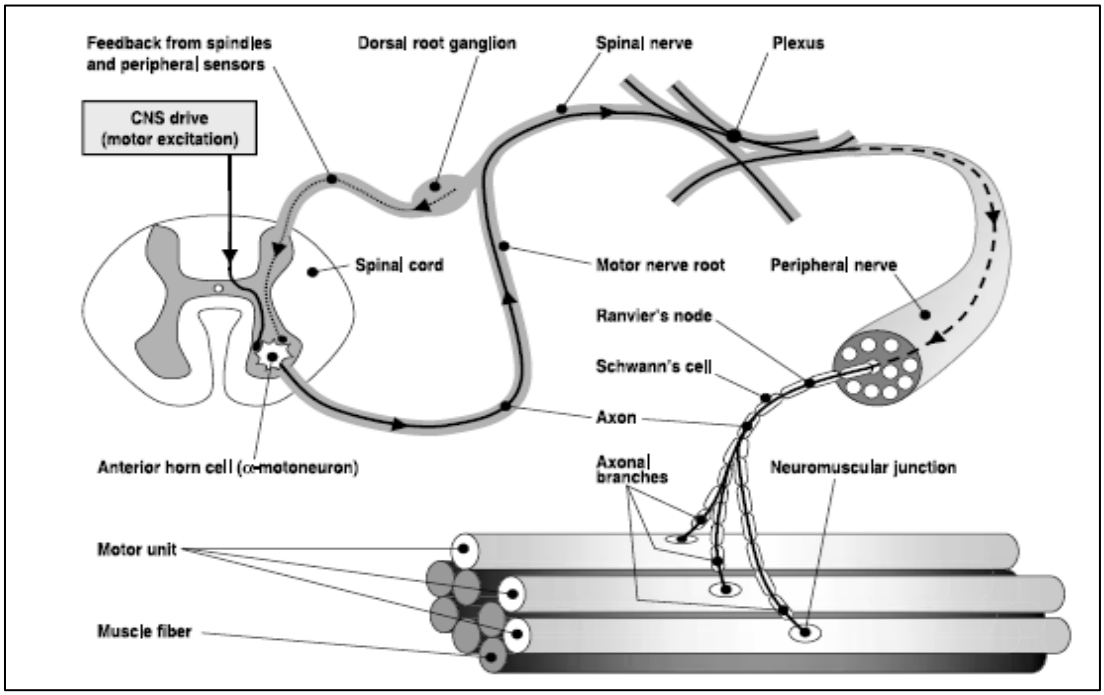

Figure 2.6: Motor unit structure. A motoneuron innervates a given number of muscle fibers at the neuromuscular junctions (Sherrington, 1929).

2.3.1.2 Physiology of muscle contraction

Normal voluntary muscle contraction begins when electrical signals, in the form of action potentials, are sent from the brain through the spinal cord along nerve cells to the motor neuron that innervates several muscles fibers to making them contract leading to the production of a movement (Fig 2.4). At the muscle, chemicals released by the motor neuron stimulate the internal release of calcium ions from stores within the muscle cell (Fig. 2.5). These calcium ions then interact with muscle proteins within the cell, causing the proteins (actin and myosin) to slide past one another. This motion pulls their fixed ends closer, thereby shortening the cell and, ultimately, the muscle itself. Recapture of calcium and unlinking of actin and myosin allows the muscle fiber to relax.

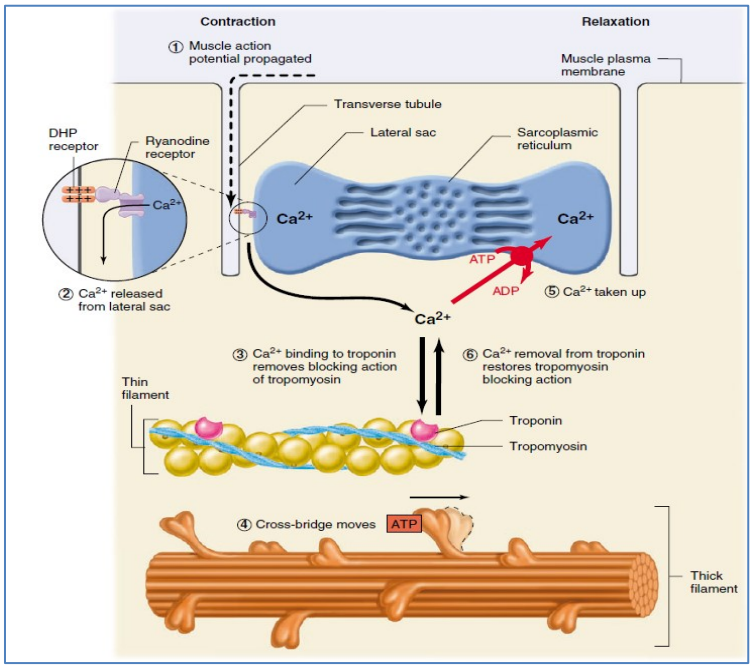

Figure 2.7: Release and uptake of calcium by the sarcoplasmic reticulum during contraction and relaxation of a skeletal muscle fiber (Widmatier et al., 2011, p.280).

Voluntary muscular contractions classified according to either length changes or force levels. In isometric contraction, the muscle remains the same length. An example would be holding an object up without moving it; the muscular force precisely matches the load, and no movement results. When a subject resisting a pull toward the back direction (back bending), the left and

right muscular activity will be equal. While for resisting a pull in the left or right direction (left or right bending), higher muscular contraction of the opposite side to the pull will be generated.

2.3.1.3 The volume conductor

On a limb or on the trunk, a biological medium separates the muscular signals from the surface electrodes. Propagation of the signal through this volume conductor is due to an electric field created by the ionic movements at the origin of the contraction. The volume conductor acts as a low-pass filter on the signal (Stegeman et al., 2000; Merletti and Parker, 2004). This filtering is much less important when intramuscular electrodes are used since they are positioned closer to the source of the signal (Merletti and Parker, 2004). Moreover, subcutaneous fat has a negative impact on surface EMG signal amplitude; it increases the separation between the electrical source (the muscle fibers) and the recording electrodes, causing decrease in surface EMG amplitude. Also it reduces the relative differences in the distances between the muscle fibers of interest and the electrodes located above the different muscles, causing the action potentials to appear more similar at each electrode (Lowery et al., 2002a).

2.3.1.4 Detection of surface EMG signal

Use of EMG is frequent in research and in numerous clinical fields such as rehabilitation medicine, ergonomics, sport, space medicine and neurophysiology (Merletti and Parker, 2004). Following its capture by the electrodes, the EMG signal is amplified, filtered, digitized and stored on a computer before further processing (Fig 2.8).

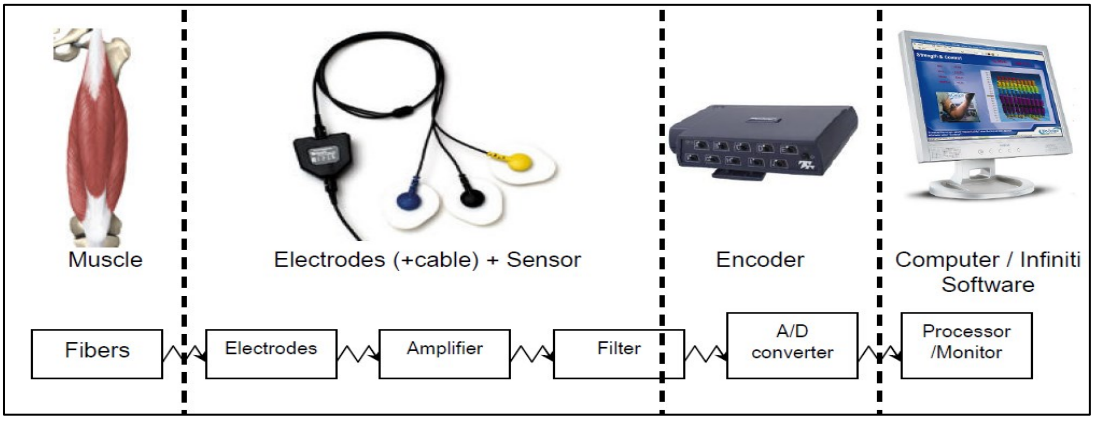

Figure 2.8: Block diagram for recording and processing surface EMG signals (Florimond, 2008)

To facilitate comparison between the EMG results obtained from various laboratories, efforts have been devoted to the normalization of the signal acquisition and processing techniques (Basmajian and De Luca, 1985). The most significant one is the work done by the European Community within the European Concerted Action SENIAM (Surface Electromyography for the Non-Invasive Assessment of Muscles) in 1999 (Hermens et al., 1999). A summary of the recommendations of this group is presented in Table 2.1.

Table 2.1: Summary Table of SENIAM Recommendations (Hermens et al., 1999)

Parameter	Recommended Value or Condition
Electrodes (bipolar montage)	
Electrode size	Diameter < 10 mm
Interelectrode distance (IED)	< 20 mm or < $^1/_4$ the muscle length, whichever is smaller
Electrode location	Between the most distal innervation zone and the distal tendon or between the most proximal innervation zone and the proximal tendon; not over an innervation zone
Reference electrode location	Wrist, ankle, processus spinosus of C7, or other electrically inactive area
Amplifier	
High-pass filter (low frequency cut-off)	
for EMG spectral analysis	< 10 Hz
for movement analysis only	10–20 Hz
Low-pass filter (high frequency cut-off)	
for general applications	~ 500 Hz (sampling frequency > 1000 samples/s)
for special wide band applications	~ 1000 Hz (sampling frequency > 2000 samples/s)
Input referred voltage noise level	< 1 μV_{RMS} (in the 10–500 Hz bandwidth)
Input referred current noise level	< 10 pA_{RMS} (in the 10–500 Hz bandwidth)
Input impedance	> 100 MΩ (for conventional electrodes) > 1000 MΩ (for pasteless "dry" pin electrodes)
Gain	suitable to bring the signal into the input range of the A/D converter with desired input resolution
Sampler and A/D converter	
Sampling frequency	> 1000 samples/s (general applications) > 2000 samples/s (wide band applications)
Number of bits of A/D	12 (requires amplifier with variable gain) 16 (fixed gain amplifiers may be used)

2.3.2 EMG Electrode Choice

Surface electrodes are very appropriate for large superficial muscles while needle or fine-wire intramuscular electrodes are used when activity of deep or overlaid muscles are to be analyzed (Türker, 1993). With surface EMG (SEMG) the detected information is collected from a greater proportion of the muscle than when intramuscular electrodes are used. SEMG is therefore more

representative of a muscle activity than the localised and selective needle electrodes (Sirca and Kostevc, 1985). Surface electrodes commonly used are of 2 types:

- **Gelled electrodes** using an electrolytic gel as a conductive interface between the skin and the metallic element of the electrode. Ag/AgCl is the most common composite for the metallic part of gelled electrodes. The Ag/AgCl layer allows ionic current of the muscle to be transformed in an electronic current. Non-polarizable, Ag/AgCl material is used in over 80% of surface electrodes (Merletti and Parker, 2004).

- **Dry electrodes** in direct contact with the skin, mainly used in applications where geometry or size of electrodes does not allow gel.

2.4 Duchenne Muscular Dystrophy and EMG

EMG has an important role in the evaluation of neuromuscular diseases. For pathological problems, MUAP analysis and evaluation of the recruitment pattern provide useful information to evaluate normal and abnormal situations and distinguish between neurogenic or myogenic disorders (Kimura 1989; Sethi and Thompson 1989; Daube 1991; Stålberg et al., 1996). Myopathic changes can be monitored with intramuscular electrodes: in general small MUAPs and polyphasic signals of shorter duration are obtained, as compared to a healthy muscle (Shapiro & Specht, 1993). While the best method for detecting X-linked gene for muscular dystrophy is estimation of serum creatine kinase (CK), Van den Bosch (1963) considered that quantitative EMG was a valid method for improving carrier detection. Until 1968, many tried his technique but failed to reproduce his findings. But Gardner-Medwin in 1986 obtained an increase of carrier detection from about 70% to 90% by using manual quantitative EMG assessment.

Later, Frascarelli et al. (1988) used the power spectrum of the EMG obtained during a sustained isometric contraction. In myopathic subjects, they found that during the isometric contractions, the total power increased. This was accompanied by a progressive increase of power in the lower frequencies with a decrease of power for the higher frequencies which resulted in a reduction of

the median frequency. As for normal children, an increase of the total power without a significant median frequency shift was noted. The modifications in the patients were explained by a reduction of the firing rate of the more damaged fast twitch MUs. This decrease was probably induced by a relative predominance of activity of the slow twitch MUs which are less damaged by the pathological process (Spencer and Eccles, 1976).

As done by various authors with normal subjects, Priez et al. (1992) quantified the evolution of DMD by investigating localized muscular fatigue during isometric contraction using spectral analysis of surface EMG. In a pilot study with DMD patients, Bowen et al. (2001) examined how the central nervous system (CSN) influence muscle activity. They linked surface EMG potentials of arm muscles to the kinematics of a point-to-point hand movement. Failure to maintain a straight hand trajectory while executing a movement was considered to indicate that the usual compensation mechanisms used to realized the desired trajectory were deficient. Unexpectedly, they found that kinematic characteristic for a point-to-point hand movement for DMD was similar to those of healthy subjects. This was explained by another recent study of 32 DMD patients where fiber conduction velocity in the biceps brachii muscle and anterior tibial muscles was measured. Compared to expected normal values, a significant smaller velocity was found, probably due to the small size of the regenerated and splitted fibers. There was also a multi-peak frequency distribution of the velocities indicating a great variability in the diameter of the muscle fibers (Stegman et al., 2000).

2.5 Muscles and Scoliosis

Many researches have been conducted to study the contribution of the muscular system on the pathogenesis of scoliosis: disturbance in growth of paravertebral muscle (Perdriolle et al., 1993). Abnormalities have been detected in: muscle spindles (Ford et al., 1987), fiber types and individual muscle fiber morphology (Fidler, 1974, Sahgal et al., 1983; Zetterberg et al., 1983), histochemistry (Spencer and Zorab, 1976) and EMG signal characteristics (Reuber et al., 1983; Butterworth et al., 1969; Gaudreault et al., 2005; de Oliveira et al., 2011).

2.5.1 EMG and Scoliosis

The first EMG investigations of the ES muscles were first reported on 1951. Since that time, several studies concerning the analysis of those muscles in relation to scoliosis have been done (Hopf et al., 1998) and most of the time an increased ES activity was reported on the convex side of the scoliotic curvature (Zetterberg et al., 1984; Thouin, 2005; Cheung et al., 2005). For some authors, such results indicate a muscular weakness on one side (Zuk, 1962; Clague et al., 1995), while for others it resulted from the stretching of the muscles on the convex side (Butterworth and James, 1969). On other hand, other studies reported that no significant differences were found in EMG amplitudes between convex and concave sides at the apex of the curvature in AIS (de Oliveira et al., 2011; Gaudreault et al., 2005; Reuber et al., 1983).

EMG imbalance may be influenced by specific exercises rehabilitation program for scoliosis which led to a highly significant reduction of the Cobb angle, as reported by Weiss et al. (2003). Valentino et al. (1985) see the asymmetry as a symptom for possible progression of the deformation, In the same direction, Cheung et al. (2005) considered that asymmetric patterns in EMG at the deviation inferior limit vertebra is associated with an eventual progression of the scoliosis. Cheung et al. (2004) also reported that when convex/concave EMG ratio of 1.25 is present, there is a 68.9% chance for a curve progression.

Bassani et al. (2008) used surface EMG for assessing neuromuscular efficiency and localized muscle fatigue in the lumbar extensors of scoliotic individuals. Their subjects underwent a fatigue induction test on their lumbar extensor muscles, consisting of one maximum voluntary isometric contraction (MVIC) followed by a test at 80% of the MVIC effort. Force and EMG signals were collected simultaneously. The results indicated that by comparing the localized muscle fatigue indices, significant differences between the scoliosis and control groups were only shown for the right longissimus muscle which showed lower fatigue indices, while localized muscle fatigue indices of the other muscles (left longissimus, right iliocostalis and left iliocostalis) did not differ significantly. The neuromuscular efficiency and strength values were 42.6% lower in scoliotic patients than in the control group. Moreover, symmetric neuromuscular activation between the right and left sides of the trunk of scoliotic patients were recorded.

In spite of those different interpretations, it is still not clear whether the reported EMG findings reflect a primary neuromuscular factor causing scoliosis or whether they only indicate a secondary mechanism induced by the deformed spine (Cheung et al., 2005).

2.5.2 Histopathology Studies

Muscle fiber types can be broken down into two main types: slow twitch (type I) muscle fibers and fast twitch muscle fiber (type II). Type I fibers are identified by slow contraction times and very resistance to fatigue, while type II generally produce the same amount of force per contraction as slow muscles, but they are able to fire more rapidly and fatigue more quickly. They are much better at generating short bursts of strength or speed than slow muscles (Herbison et al., 1982).

A greater proportion of type I fibers, on the convex side is consistently reported but the real significance of this result is difficult to assess due to the lack of knowledge of the fiber type distribution in those muscles (Bylund et al.,1987; Bogdanovich et al., 2004). In young women the major scoliotic curve is often located in the thoracic region but there is not much information on healthy backs, especially with regards to women and to muscles in the thoracic region (Gaudreault et al., 2005). It is thus difficult to explain the aetiology of this disease through the alteration of muscle fibers.

In 1976, Spencer et al. were the firsts to study muscle fiber types in AIS. They noted a decrease of type II fibers in AIS patients suggesting a denervation or myopathic process. As for Fidler et al. (1976), it was reported in AIS that there was a greater numbers of types I fibers on the convexity at the apex and atrophy of type II fibers on the concavity at the apex of the curve. Sahgal et al. (1983) found on increased number of type I fibers on both sides of the curve in AIS as well as in the gluteus medius.

When a comparative study of the ES muscles of AIS patients and healthy age matched controls was made, Bylund et al. (1987) reported that there was a significantly greater relative proportion of type 1 fiber on the convex side (75.4%) than on the concave side (57.7%) in the AIS girls. In comparison, the type I fiber distribution on the concave (left) side was smaller than for the AIS

than for the healthy girls (respectively 57.7% vs 67.5%) while the convex (right) side of the healthy and AIS were similar. However, three AIS boys group showed the same difference in relative proportion of type 1 fiber difference between the convex and concave sides as for girls AIS group. In double primary curves, the same distribution of type I fibers was seen in both curves. The authors concluded that in AIS there is a normal distribution of type I and type II fibers on the convex side but a lower number of type I fibers on the concave side.

In 1987 Ford et al. did a histologic and histochemical analysis of the distribution of muscle spindles in ES muscles of AIS patients. Muscle biopsies were taken from the apex of the primary curve, as well as two levels above and below the curve, and on both the concave and convex sides. They noted a marked decrease in muscle spindles in all paraspinous muscles tested on both sides in AIS patients.

Mannion et al. (1998) studied the extent to which the paraspinal muscles are affected in idiopathic scoliosis and whether one side at the apex of the scoliotic curve showed greater muscular abnormalities than the other. Paraspinal muscles samples were obtained from 14 female scoliosis patients, at the apex of the scoliotic curve at T9-T11. Compared with control muscle, there was a significantly lower proportion of type I (slow-twitch oxidative) fibres in the muscle on the concave side of the scoliotic curve, but no difference on the convex side. The proportion of type IIB (fast-twitch, glycolytic) fibres was higher on both sides of the curve compared with controls, with the effect being significantly more marked on the concave side. The percentage of type IIA (slow-twitch, oxidative-glycolytic) fibres did not differ between the groups, and neither did fibre size. They reported that the spinal musculature is most affected on the concave side at the curve's apex in scoliosis. So, when one looks at the muscle fiber composition of scoliotic subjects, it is important to check on which side of the spinal curve the information is applicable.

2.6 Scoliosis in Friedreich's Ataxia

Patients with FA develop scoliosis with a prevalence of 63% to 100% (Milbrandt et al., 2008; Cady and Bobechko, 1984). The natural history and treatment of FA scoliosis is limited due to the rarity of the condition. Previous reports have described the progression, curve patterns and

treatment of the FA scoliosis (Cady and Bobechko, 1984; Labelle et al., 1986; Daher et al., 1985). While some classified it as a neuromuscular scoliosis (Milbrandt et al., 2008) similar to that seen in muscular dystrophy characterized by long C-shaped curves associated with pelvic obliquity and severe muscle weakness, others see it as an AIS with greater incidences of double major curve patterns, single thoracic and thoracolumbar curves (Labelle et al., 1986). Cady and Bobechho's (1984) found only 3 of their 42 patients had a C-shaped curve with pelvic obliquity; Daher et al. (1985) had none in their series, while Labelle et al. (1986) found 14% had a neuromuscular-type curve pattern. FA scoliosis is frequently associated with hyperkyphosis. This feature was seen in 42% of Daher et al. (1985) patients and in 66% of patients in the series of Labelle et al. (1986).

Moreover, Labelle et al. (1986) found that scoliosis in FA patients is not always progressive and no significant correlation established between over-all muscle weakness and curve progression. So, they hypothesized that the pathogenesis of FA scoliosis is not related to muscle weakness but results from the perturbations in the proprioceptive and balance systems. Similar findings were reported by Aronsson et al. (1994) who saw no correlation between the severity of the curvature and muscle weakness or functional status and supported the concept that the underlying causes of AIS and FA scoliosis are similar, since both disorders have similar curve shapes.

For FA patients with a progressive scoliosis, Labelle et al. (1986), reported that all of them the onset of the disease or its recognition was before their growth spurt, and the progression of the curve appeared more severe while the growth spurt continued suggesting that skeletal immaturity is a key factor in the development of the deformity. For Cady and Bobechho's (1985), the scoliotic curves tend to progress with the severity of the disease and progression can continue beyond skeletal maturity. Based on the length of the spines of fifty-three patients with FA, Allard et al. (1982) used a three-dimensional geometric reconstruction program and found that the maximum growth spurt in FA patients occurs between the age of ten and fifteen in girls and between twelve and seventeen in boys. While Allard et al. (1982) recommended bracing for curves of 20-40° in growing children, many authors disagree. Cady and Bobechho's (1985) found that 5 patients treated in braces all progressed an average of almost 11° per year. They concluded that braces are not indicated as they are unable to control the curves and they

sometimes cause additional problems with these patients with progressive ataxia and muscles weakness. Daher et al. (1985) reported that in 19 patients with FA scoliosis, treatment with a brace was unsuccessful. Milbrandt et al. (2008) got the same results.

As a treatment protocol for scoliosis, Labelle et al. (1986) recommended that children with a Cobb angle of 40° or less should be observed but not braced, while curves of 40-60° needed to be observed for progression and if it occurs, fusion should be considered, since with surgery, the curve angle is reduced and better balance is possible. Some authors recommended posterior fusion with Harrington rod instrumentation and segmental wiring, if the curve progressed beyond 40°, but no results of surgery were given (Allard et al., 1982). Milbrandt et al. (2008) found that fusion using modern segmental constructs was effective in creating substantial intraoperative correction and maintaining correction postoperatively. Tsirikos and Smith (2012) reviewed 31 patients with FA scoliosis. They reported that due to post-operative complications, one patient died due to a cardiorespiratory failure.

2.7 Ultrasound Imaging

The use of this non-ionizing and non-invasive real time imaging approach has rapidly expanded, leading to its widespread use in almost all fields of medicine such as obstetrics, gynaecology, orthopaedics, cardiology, and urology. It is also getting more frequently used for the diagnostic of neuromuscular disorders (NMD).

An ultrasound (US) system includes a transducer (probe) which generates a high frequency sound wave (2-20 MHz or 0.8-0.08 mm wavelength) which can travel through soft tissues such as muscles and internal organs. The probe is made of many piezoelectric elements which convert electrical energy into sound energy and vice-versa. When an interface is encountered (e.g., interface between muscle and bone), the sound wave is partially reflected, whereas the rest of the sound energy is transmitted to deeper layers. The reflected sound wave is detected by the piezoelectric elements which convert it in an electrical signal which is processed to produce in real time an image of the tissues under the probe (Coatney, 2001).

A penetration of up to 15 cm is possible with the use of low frequencies but the resolution is low (several mm). When a higher frequency is used, the penetration depth is less (only a few cm) and the resolution is higher (≤1 mm). As the US signal travels through the body, it loses its energy through absorption, scatter and reflection phenomena and this is known as attenuation. The attenuation being greater with higher frequency, the penetration is thus less (Hughes, 2001).

Resolution of an US image is measured axially (depth along the beam) and laterally (transversely across the beam). The axial resolution is directly related to the frequency of the transducer; at best, it approaches the wavelength of the sound emitted by the transducer. For muscles studies, 5 or 7.5 MHz probes are usually recommended as they ensure sufficient depth penetration (Zsidai, 2001).The lateral resolution of US is limited by the beam width of the probe and is several times larger than the axial resolution (Hughes, 2001).

An US system needs a central processing unit (CPU) to control and execute all the functions of the system. The CPU is thus used for the communications between system components such as the transducer and monitor and the creation of an image from all returning echoes is based on an analysis of the temporal and acoustic properties of the echoes. The amount of returning echoes per square area determines the gray value of the image, that is, echo intensity. The time between sending and receiving the US pulse determines the location of the corresponding pixel; it is also used to calculate the depth of the tissue interface causing the echo, whereas the brightness of the image corresponds to the amplitude of the sound wave (Hughes, 2001). Software programs are used to make quantitative measures on the images and to store them (Coatney, 2001).

2.7.1 Imaging techniques and muscular diagnostic

As shown in Table 2.3, each imaging approach is more appropriate in a given situation. MRI is capable of detecting NMD especially in adults and in patients with inflammatory myopathies, but no prospective studies has yet been performed to detect its efficiency on children. However, MRI is less capable of detecting pathological changes in early or pre-symptomatic disease, and in metabolic or mitochondrial myopathies. Although computed tomography (CT) is capable of detecting fatty infiltration caused by NMD and appears to be superior to MRI in detecting

calcifications caused by inflammatory myopathies, there is no data on the predictive value of muscle CT in the diagnosis of NMD.

MRI has been used by Zoabli et al. (2008) to analyze ES muscles in scoliotic spine in few DMD patients. It has been shown that the volume of the ES muscle of pre- and scoliotic patients was found smaller on the convex side relative to the concave one. While, the fat infiltration was found larger on the convex side of pre- and scoliotic patients and no significant difference was observed in non-scoliotic patients.

Table 2.3: Advantages and disadvantages of muscle imaging technologies (Clague et al., 1995)

Variables of Imaging Technologies	Ultrasonography	Computed Tomography	Magnetic Resonance Imaging
Availability	Readily available	Readily available	Increasing
Cost	Inexpensive	Expensive	Very expensive
Portability	Portable	Fixed	Fixed
Soft tissue contrast	Fair	Good	Excellent
Muscle detail	Fair	Good	Very good
Safety	Excellent	Ionizing Radiation	Excellent
Time to acquire image	Real time (ms)	Long (seconds to minutes)	Long (minutes to hours)
Spatial resolution	1-2 mm	<1 mm	<1 mm
Temporal resolution	Tens of ms	Hundreds of ms	Seconds

A deficit in the number of muscle fibers on one side of the spine due to a larger fat infiltration is a factor that can contribute to the presence of uneven forces on the spine, leading to its deformation. While uneven forces could also result from the action of the CNS on those muscles, such action seems to be different between the pre- and scoliotic stages. As for Hides et al. (1995) a comparison was made between MRI and US of the lumbar multifidus muscles and no significant difference was found. Those authors concluded that real time US can be used to document muscle size in young adults.

While both MRI and CT can visualize deeper located muscles than US, this latter approach has still the major advantages of being radiation-free and less expensive than MRI. Also, with its high temporal resolution (>0.1 ms) US allows dynamic imaging of contracting muscles (Pillen, 2010).

Modern US equipment is capable of producing 3D images at a high acquisition rate (between 10-60 images/s). So, within a single breath hold, it can greatly increase modeling accuracy of organs which move with inspiration and expiration. This also allows the study of organ motion itself; much of the development of 3D ultrasound has been targeted towards such cardiac studies. Shorter examination times are also beneficial for clinicians and patients (Treece et al., 2001). When the musculoskeletal system is under study, skin, subcutaneous fat, ligaments, tendons, muscles and bones are all components with different acoustic properties which affect the produced US images.

2.8 Ultrasound and Duchenne Muscular Dystrophy

It was in 1980 that different patterns were detected between diseased and healthy muscles with US imaging (Zuberi et al.,1999). Since then, it has been shown many times that US can be used to detect and distinguish between NMDs, including muscular dystrophies, inflammatory myopathies, etc. (Lamminen et al., 1988; Heckmatt et al., 1982; Zaidman et al., 2010; Jansen et al., 2012). NMDs usually lead to changes in muscle morphology which are detected by measuring muscle size, subcutaneous tissue thickness, muscle echo intensity (echogenicity), muscle inhomogeneity and grey-area index.

Normal muscle tissue appears as a structure with low echo intensity (relatively black picture) since it contains only few fibrous tissue on which reflections can occur. Its boundaries are clearly visible and thus easily discerned from subcutaneous fat, bone, nerves, and blood vessels; as for pathological muscles, they show increased overall echogenicity or increased inhomogeneity due to disruptions of their architecture (Maurits et al., 2003). As we can see in Fig. 2.9b, in DMD patients, replacement of muscle tissue by fat and fibrous tissue leads to a disruption of the pattern seen in a normal muscle (Fig.2.9a).

Quantification of muscle echo intensity has been reported in many studies. For instances, Heckmatt et al. (1982) developed a visual grading scale to describe the extent of alterations on US in which grade I represented normal muscle and grade IV severely increased muscle echo intensity with total loss of bone. Heckmatt et al. (1989) also reported 84% sensitivity based on density analysis in children with DMD, while Zuberi et al. (1999) using the same qualitative

criteria of Heckmatt et al. showed a higher percentage of sensitivity could be reached in NMD children older than 3 years while the test was less reliable in younger children (i.e. ≤3 years).

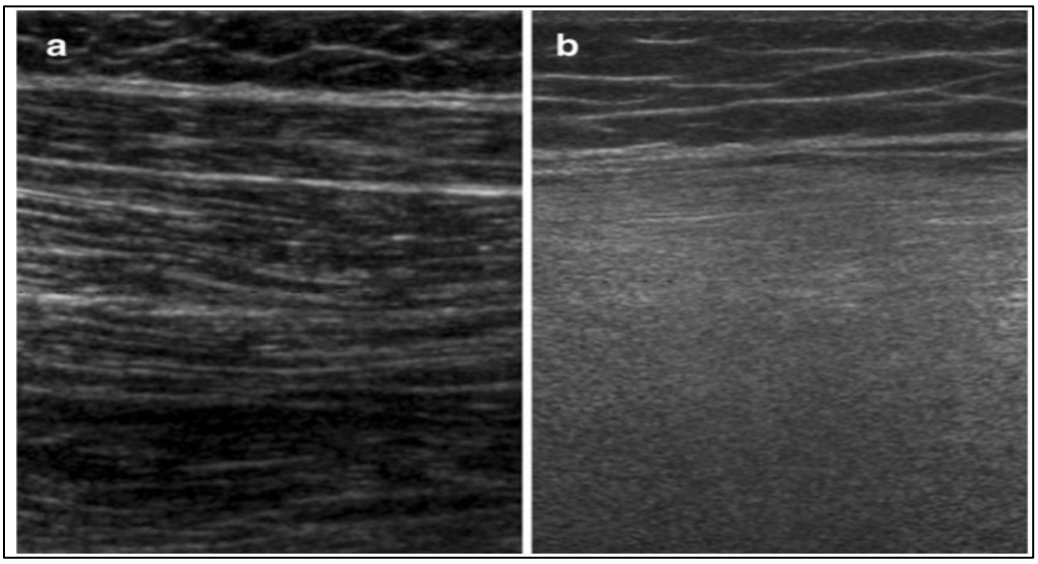

Figure 2.9: a) Ultrasound images of the quadriceps muscle in normal subject where muscle appears largely black with few perimysial septa. b) Image of a DMD patient where the increased homogeneous fine granular echogenicity is due to the replacement of muscle fibers by connective and fatty tissue (Wattjes et al., 2010).

2.9 Ultrasound and Scoliosis

To our knowledge, US images to characterize the paraspinal muscles in AIS patients have been used in only few studies to our knowledge. In 1993 Kennelly and Stokes examined the symmetry of lumbar multifidus size in 20 AIS patients. Cross-sectional area (CSA) and linear (horizontal and vertical) measurements were made on bilateral real-time US images obtained at 4th level of the lumbar vertebra (L4). Asymmetry of lumbar multifidus cross sectional area were detected for different curves types and it was concluded that these preliminary findings supported further investigation of the role of the musculature in the pathogenesis of AIS. While those results may be applicable to scoliosis of neuromuscular origin (muscular dystrophy), no such patients were included in the study. Purnama et al. (2009) recently investigated US as an alternative way to image the human spine in order to follow scoliosis progression (Fig. 2.10). A freehand 3D US

system was used to scan the back of normal subject. From their results, it seems possible that the progression of a scoliotic curve could be detected with US imaging.

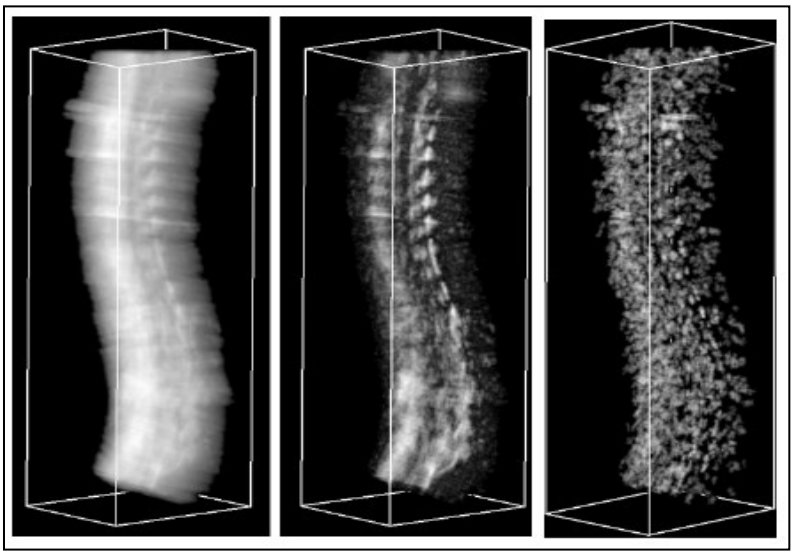

Figure 2.10: The reconstructed ultrasound volume (left), after filtering to remove non-vertebral features (middle and right) (modified from Purnama et al., 2009).

Chapter 3: Methodology

3.1 Patients and Subjects

Eight young teenagers protocol aged 10-16 years with body mass index (BMI) ranges from 13.6 to 22.8 were enrolled in the experimental protocol. Four scoliotic FA patients, 3 with right spinal deviation and one with left spinal deviation, were recruited from the neuromuscular disease clinic of Marie-Enfant hospital. As a control group, 4 healthy young boys with matching BMI and structurally normal spines were chosen. Information on each subject is provided in Table 3.1.

Table 3.1: Some characteristics of the 4 control subjects and the 4 FA patients

	#	Age (years)	Weight (kg)	Height (cm)	BMI (kg/m^2)	Cobb angle (°), position	Status	Sex
Control subjects	C1	14	56	167	20.1	-	Healthy	Boy
	C2	11.5	42	150	18.7	-		Boy
	C3	12	47	155	22.8	-		Boy
	C4	13	69	174	22.8	-		Boy
	Mean	12.6±1.1	53.5±11.8	161.5±11	21.1±2.04			
FA patients	P1	10	24	125	15.4	40°(R)	Ambulant	Girl
	P2	13	47	155	22.8	18°(R)	Ambulant	Boy
	P3	16	45	182	13.6	30°(R)	Non-ambulant	Boy
	P4	12	32	135	17.6	32°(L)	Non-ambulant	Boy
	Mean	12.7±2.5	37±10	149.3±25.1	17.3±4			

FA patients were either ambulant or wheelchair-dependent but were able to stay in a sitting position on a backless bench. They participated in the study even if they were taking medication, but those having undergone a spinal surgery were excluded. Written, informed consent was obtained from each subject's parent before starting the experiment. The protocol had been approved by the Sainte-Justine Hospital's Ethic Committee (Appendix A).

3.2 Experimental Protocol

3.2.1 EMG

The EMG signals were acquired while the patients were sitting on a low back chair (Fig. 3.1). An inextensible harness was put at the shoulder level and linked to a fixed point through a steel cable. A strain gauge (PAXLSG, Red Lion Controls) was inserted between the cable and the point of fixation and its display was positioned in front of the subject who used the reading as a feedback signal to keep the force constant over the 5 s duration of each trial.

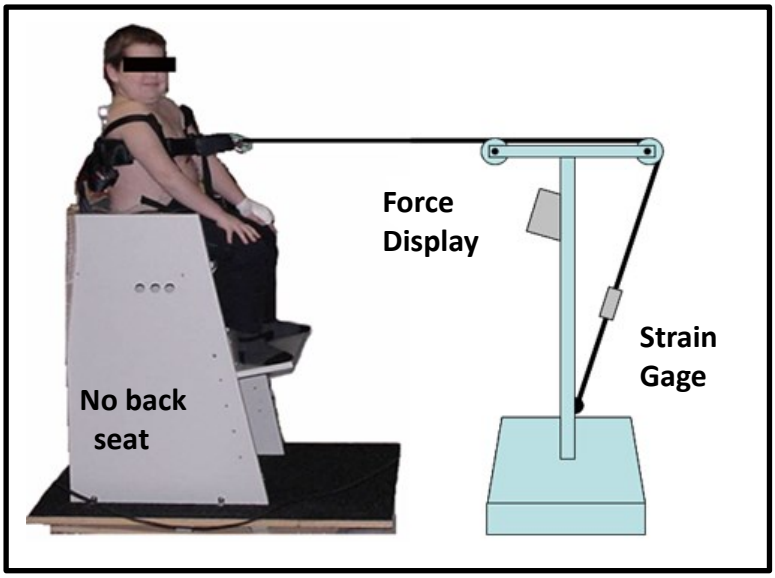

Figure 3.1 : EMG Experimental set-up (Thouin, 2005).

First the skin was cleaned with alcohol swab to reduce skin impedance, prior to the surface electrodes placement. A marker pen was used to identify the position of the vertebrates from the top to the bottom of the scoliotic curve and 5 pairs (bipolar recording) of disposable Ag/AgCl surface electrodes (Nutab^{TM}, King Medical Ltd, King City, Canada) with a 20 mm center-to-center distance were bilaterally attached parallel to the muscle fibers on both sides of the trunk at levels T10, L1 and L5 at 25 and 50 mm from the spinal processes (Fig 3.2). Bilateral recording of the rectus abdominis was also done as well as the electrocardiographic (ECG) signal through a pair of electrodes placed near the sternum. The ECG signal was used to filter cardiac activity

from EMG signals when necessary. The reference electrode for the EMG system was positioned over the elbow.

The subjects had to perform three tasks: back bending (resisting to a front pull), right bending (resisting to a pull to the left) and left bending (resisting to a pull to the right). The right and left bending tasks were done to detect if a general pattern in muscular activity was present and if yes, to observe how scoliosis could interfere and modify the pattern. For each of these tasks the maximum voluntary contraction (MVC) was determined by the mean value of 3 maximum contractions accomplished by the patient. The subjects were asked to perform contractions at a level corresponding to 20% and 100 % of the MVC established for each of the 3 tasks. Each 5 s-long contraction was repeated 3 times at the 2 levels of contraction and for the 3 directions of the pull. To prevent fatigue, a rest of 30-60 s was taken between each contraction. To evaluate the noise level and the stability of the electrode recording systems throughout the tests, EMG signals were recorded at the beginning and at the end of each experimental session while the subject was in a relaxed resting position.

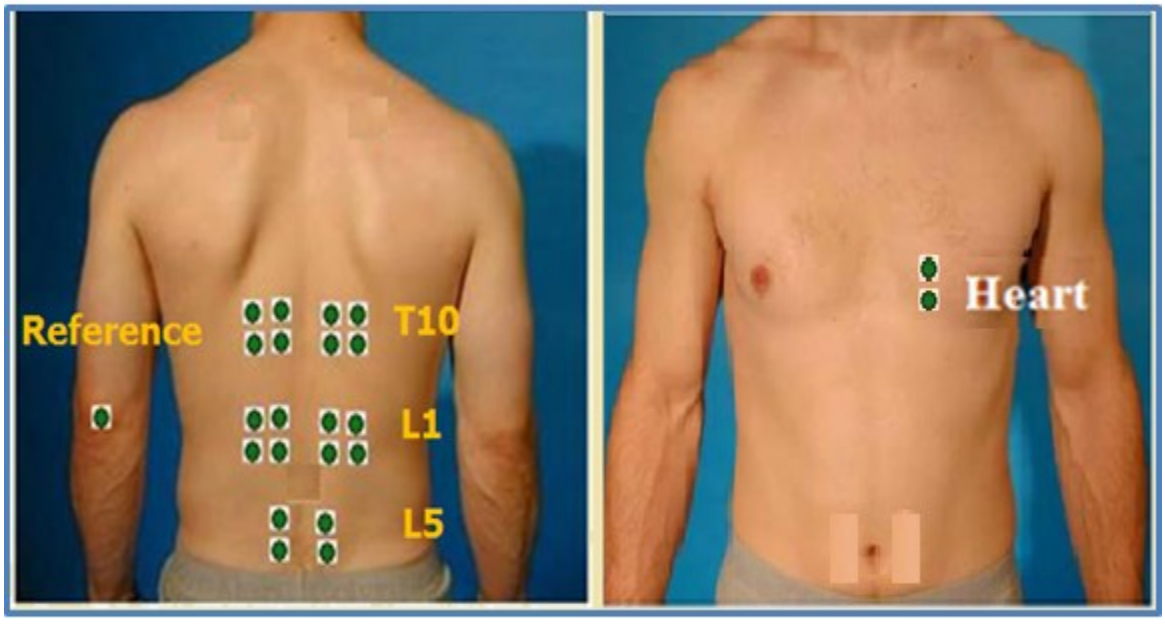

Figure 3.2 : Five pairs of surface electrodes were placed on the left and on the right of the spine at levels T10, L1 and L5 at 25 mm and 50 mm from the spine. The reference electrode was placed on the elbow (adapted from Thouin, 2005).

3.2.1.1 EMG Equipments

A 24-channels EMG system was used (model 15A54, Grass-Telefactor, West Warwick, RI, USA). For the amplifiers, a gain of 2000 and a bandpass filter of 3-1000 Hz was used. Signals were digitized online with a data acquisition card (Model PCI 6033E, National Instruments Inc., Austin, TX, USA) at 2000 Hz under the control of a user interface (Labview, National Instruments Inc., Austin TX, USA) at 2000 Hz under the control of a user interface (Labview, National Instruments Inc., Austin. TX, USA).

3.2.1.2 EMG Signal Processing

On all digitized EMG signals a notch filter was used to first eliminate 60 Hz interference. As for ECG artifacts, when a QRS complex of the ECG signal reached a pre-set threshold, a window of the EMG signal spanning essentially the length of the QRS complex was removed and replaced with a copy of the EMG signal samples adjacent to the contaminated segment. To remove baseline drifts, mean value of the EMG signal was subtracted from each EMG data point. For one subject (P3) a Butterworth band pass filter (4^{th}order) between 20-300 Hz was used to remove artifacts on his EMG signals.

Following that filtering, each 5 s recording was divided in 10 contiguous segments of 0.5 s over which root mean square (RMS) values where obtained and used to compare the signals collected over the 12 electrode pairs.

$$RMS = \sqrt{\frac{\sum_{n=0}^{N} EMG^2}{N}}$$

Within a given test, the mean of the 30 RMS values obtained for the 3 executed trials was used to represent the activity over an electrode pair. For the statistical analysis a Student t-test was used to compare activity of one muscle on one side of the spine to its counterpart on the opposite side. An Anova one-way test when all activity on one side of the spine was compared to the one on the other side. A significance level of $p<0.05$ was used with both tests.

3.2.2 Ultrasound Protocol

An ACUSON S2000 ultrasound system (Siemens Co.) was used with the linear and high density transducer 18L6 HD (depth: 4.5cm, 12 MHz, 0 dB, Map E). For image acquisition, (Fig. 3.3), the

subject was asked to lay over an experimental table in the prone position and the arms were placed near his body over the table. By palpation, the spinous process of L5 and the iliac crests were located and their location marked with a pen. Two scanning steps were used. Initially, the US probe was placed transversely over L5 in the mid-line and the spinous processes and laminae were identified on a cross-sectional scan. Then, the probe was moved laterally from L4 to T8 on each side of the spine to image the left and right ES muscles while images were being stored in the US equipment. In an off-line process, the measurement tool available on the US machine to calculate the cross sectional area (CSA) in cm^2 and the skinfold thickness (mm) were used on the recorded images.

The second step was done for the purpose of reconstructing the volume of the ES muscles. For that purpose, a position sensor was stiffly mounted on the probe for its tracking along the spine with a Polaris camera system. On each side of the spine from L4 to T8, three sweeps of approximately 100 slices (depending on the probe's speed while we were scanning the spine) were recorded using US StradWin software v4.6 (Medical Imaging Group, Eng. Dept. University of Cambridge). Images from those sweeps were stored and processed off-line with the measurement tool of StradWin software in order to reconstruct the volume of the ES muscles on each side of the spine.

3.2.1.1 3D Freehand US Equipment

An illustration of the freehand 3D imaging ultrasound system is shown in Fig. 3.3. The ultrasound Acuson S2000 is shown on the left. The computer system in which the StradWin software v4.6 (Medical Imaging Group, Eng. Dept. University of Cambridge) was used to obtain the volume reconstruction of the ES muscles is shown in the middle. The StradWin software is used to retrieve the 2D US images from the Siemens equipment and communicates with the optical tracking system (POLARIS, Northern Digital Inc., Waterloo, Canada) to gather position and orientation data. The 3D reconstruction is generated and displayed on the screen of the computer in real time. StradWin also provides essential system features such as storage and retrieval of data, 3D data interaction, reslicing, manual segmentation and volume calculation for segmented regions.

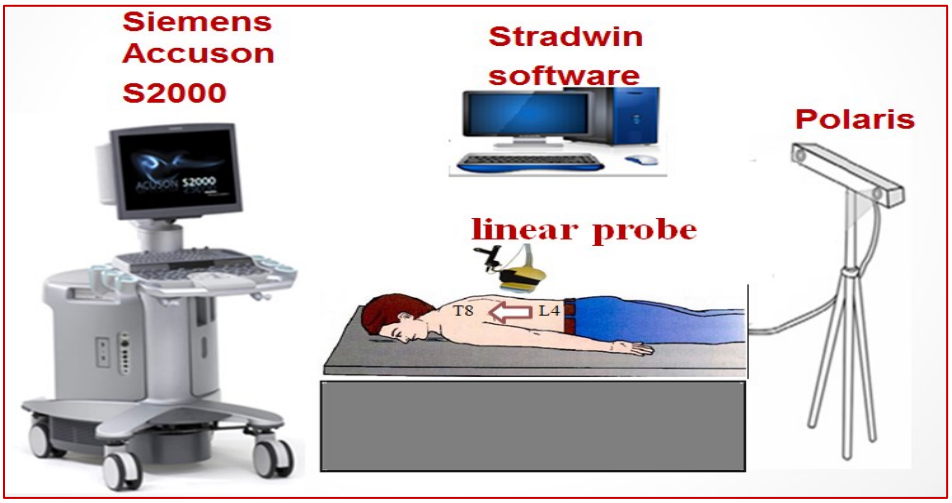

Figure 3.3: Freehand 3D US setup. The patient is lying prone on an examining table for the acquisition of the US images. The probe is moved along the spine. Images from the Acuson machine are stored as StradWin file on the computer where this software is running (on the table at the back). The StradWin software is in charge of the synchronization between the Acuson images and probe location along the patient's back with the use of the Polaris positioning system shown at the right.

The Polaris optical system can suffer from line-of-sight issues if the position sensor tool is covered or rotated away from the cameras. To minimize this problem, a Traxtal Adaptrax position sensor tool (Traxtal Inc., ON, Canada) was used. This allows a wider range of orientations of the transducer without its disappearance from view. To link the US images acquisition with the StradWin software, a video grabbing device (Belkin Hi-Speed USB 2.0 DVD Creator) was used.

3.2.2.2 Calibration

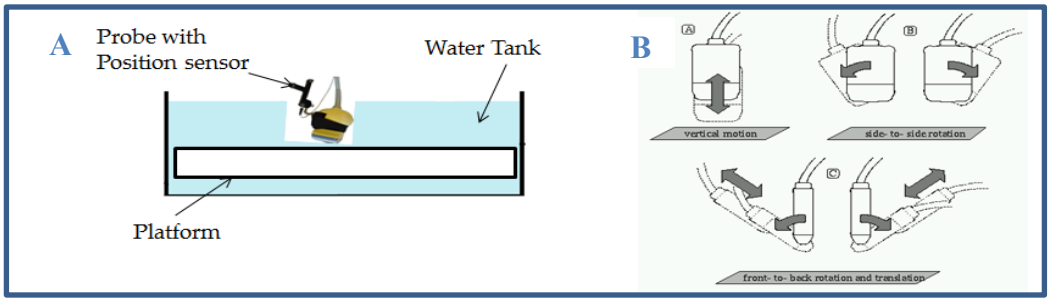

Figure 3.4: StradWin Calibration procedure. **A.** a flat-bottomed water bath with platform, the probe mounted above the phantom plane. **B**. Sequence of movements while StradWin detects lines formed by the bottom of a water bath.

Calibration is a key process for setting up a freehand 3D US system. It determines the required transforms between the coordinate systems of the US probe, the tracking device and the real world in order to be able to put the US images in a 3D dataset. For this purpose, StradWin offers a fairly simple, semi-automated calibration process in which the user sets some parameters and then goes through a series of specific probe motions while StradWin detects lines formed by the bottom of a water bath (Fig. 3.4). Calibration procedure is described in Appendix B.

3.2.2.3. Ultrasound Measurements

To get CSA (cm^2) of ES muscles, the edge of the muscle outline was followed with an on-screen cursor. To compare CSA on the patient's concave (CSAconcave) and convex (CSAconvex) sides, an index (CDI) was used:

CDI (Cross-sectional area difference index) =
{1 - (CSA concave/CSA convex)} * 100 (%).

For the skinfold thickness, the distance separating the top portion of those muscles from the skin surface over which the probe was making contact was obtained with a tool available on the US machine. For comparison purposes, a STR index (skinfold thickness ratio) was used:

Skinfold Thickness Ratio (STR) = ((concave-convex)/concave) *100(%)

A scan along the spine contained around 100 slices and the procedure was done 3 times. To determine the boundaries between each of the ES muscle in each image, a manual segmentation was done. The distance between any 2 spinous process tips served as landmarks to delimit the top and bottom of the muscle at each spinal level. From each scan, the ~100 slices were used to obtain a 3D reconstruction which was obtained with the StradWin software. From the 3 individual volumes, a mean value was obtained for each side of the spine.

Chapter 4: Results

EMG and anatomical measurement results obtained from our 4 AF patients and 4 controls are initially presented. Since the study covers only few patients with quite different Cobb angles, the results should only be considered as four cases study. To extend those EMG studies, we also included EMG data collected from DMD patients enrolled in the first study of our group with DMD patients. Those data were collected one year after a first acquisition and where not analyzed for the production of Thouin's thesis (2005).

4.1 EMG Results

4.1.1 Friedreich's Ataxia Patients

Patient 1. As illustrated in Fig 4.1, during maximum back bending task (100% MVC), EMG activity was slightly greater on concave than convex[1] for iliocostalis at T10 and L1 level as well as for long dorsal muscles at L1, while activity was slightly higher on convex than concave for long dorsal muscles at T10 level. But none of these differences are significant. For common mass muscles at L5 level, EMG activity is similar on both sides of the spine. While at 20% MVC, EMG activity was significantly higher on the convex side than on the concave one at all sites ($p<0.018$) except for iliocostalis at T10 level, where EMG activity was significant higher on the concave side than on the convex one.

During Left bending task at 100% MVC, EMG activity of convex side was higher than that at the concave side on all recording sites, and the difference was significant at T10 and L5 levels. As for a pull in the other direction, a right bending task, the amplitude of EMG activity on the convex side was twice higher than the EMG amplitude for left bending task (30.7μV & 14μV, respectively) and this was significantly higher at all levels on the convex side than on the concave one.

[1] When more EMG activity is present on one side, the effect is to push the vertebral column on the opposite direction.

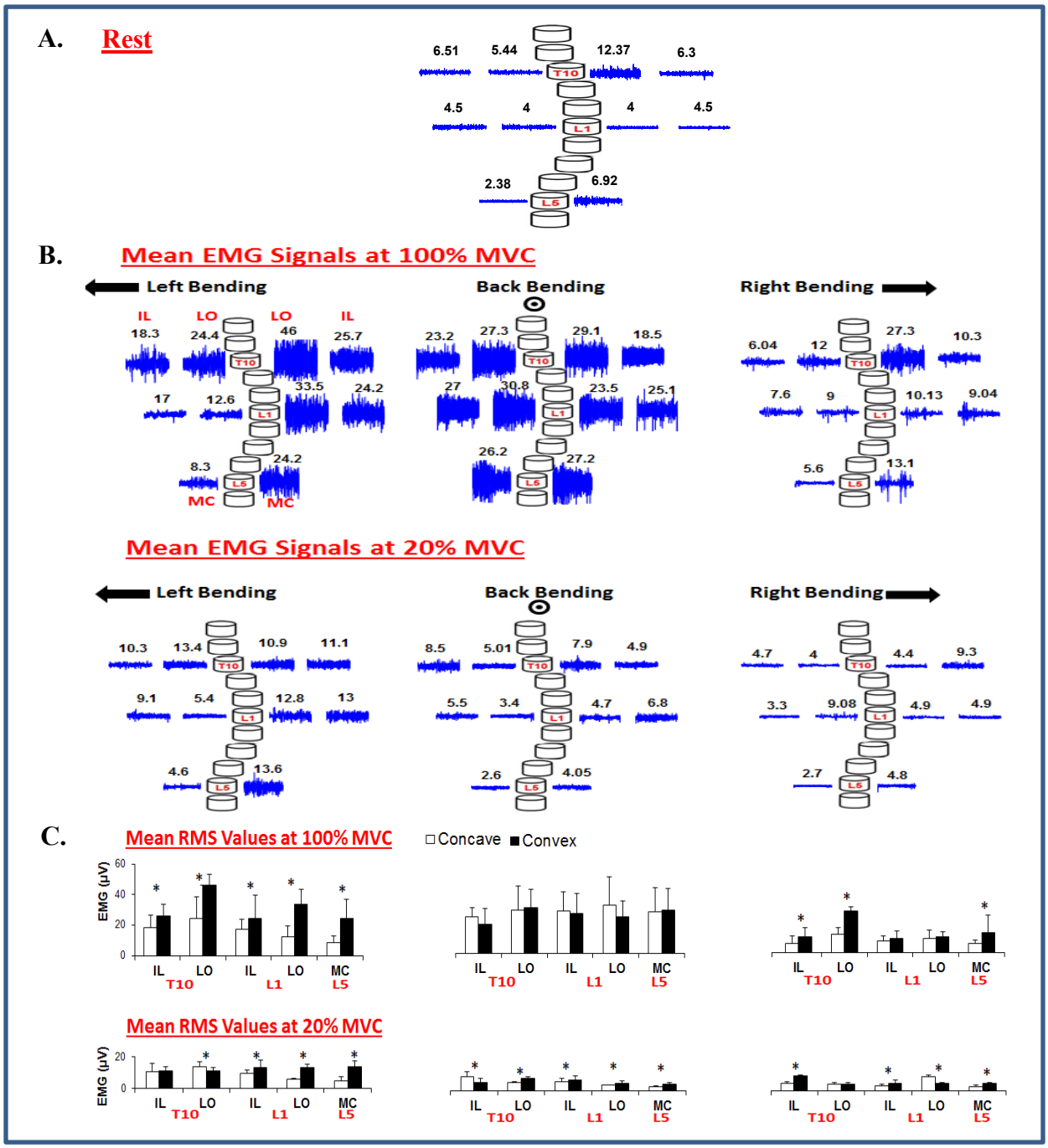

Figure 4.1 : Patient P1 (40°, R). A. EMG signals obtained at rest position. **B.** Mean EMG signals obtained from 3 trials of 5 s isometric contractions realized at 100% and 20% MVC while resisting to a pull to the right (Left Bending), a front pull (Back Bending) and a pull to the left (right Bending). Recording were made at the T10, L1 and L5 levels with the iliocostalis activity recorded at 6 cm from the spine and the longissimus activity at 3 cm from the spine. At L5, activity is from the common mass at 3 cm from the spine. **C.** means (± SD) obtained from 30 RMS values calculated on 10 contiguous 0.5 s section obtained from each set of 3 trials. Results are in black for the convex side and in white for the concave one. *p< 0.05 significance level (Student t-test).

Patient 2. During the back bending task at 100% MVC, EMG activity was significantly ($p < 0.05$) increased on the concave side of the scoliotic curve for iliocostalis and long dorsal muscles at T10 and L1 level as well as for the group of long-T10 dorsal muscles, while for common mass at L5, a small and non-significant difference on the concave side than on the convex side was observed (Fig. 4.2). When the effort corresponded to 20% of MVC of the trunk extension, the mean RMS values of the left and right sides didn't show any significantly different exception of group long-dorsal muscle at T10 level and L5 level showed a significant increase on opposite side. As for maximum left bending task, a higher significant EMG activity on the concave side of the scoliosis curve is observed at all levels on all recording site except at T10 for long dorsal muscle the difference was not significant. As for a pull on the other direction, activity was significantly higher at all levels but on his opposite side. At 20% MVC of left bending, when all back signals on one side of his spine were grouped, the activity of paraspinal muscle were found similar (7.63μV for left and 7.51μV for right). While at 20% MVC of right bending, EMG activity was significant higher on the concave side than on the convex side for long dorsal muscles and iliocostal groups at T10 level and at L1 level and muscular activity was found similar on both sides of the spine at L5 level.

Patient 3. During the back bending task at 100% MVC, EMG activity was found higher on the concave side than on the convex side at all recording sites. It was significantly ($p < 0.001$) increased on the concave side of the scoliotic curve for iliocostal and long dorsal muscles at lumbar level (Fig. 4.3). When the effort was correspondent to 20% of MVC of the trunk extension, the mean RMS values of the left and right sides were almost similar, we didn't detect any significantly different exception at L5 level showed a significant increase on the concave side than on the convex one ($p < 0.001$).

Patient 4. This patient was the only one who had a left scoliosis of Cobb angle 32º. As shown in the figure 4.4 below, amplitude of his EMG signals was very low (3.5μV) due to his inability to produce force and due to his high level of skin fold thickness. When all back signals on one side of his spine were grouped, a significant difference was found between the activity of his left (convex) and right (concave) paraspinal muscle. Higher muscular activity was observed on the convex side than on the concave one at 100% and 20% MVC during back and left bending task.

However during right bending task, EMG acquisitions showed no imbalance at the paraspinal muscle activity between left and right at 100% and 20% MVC.

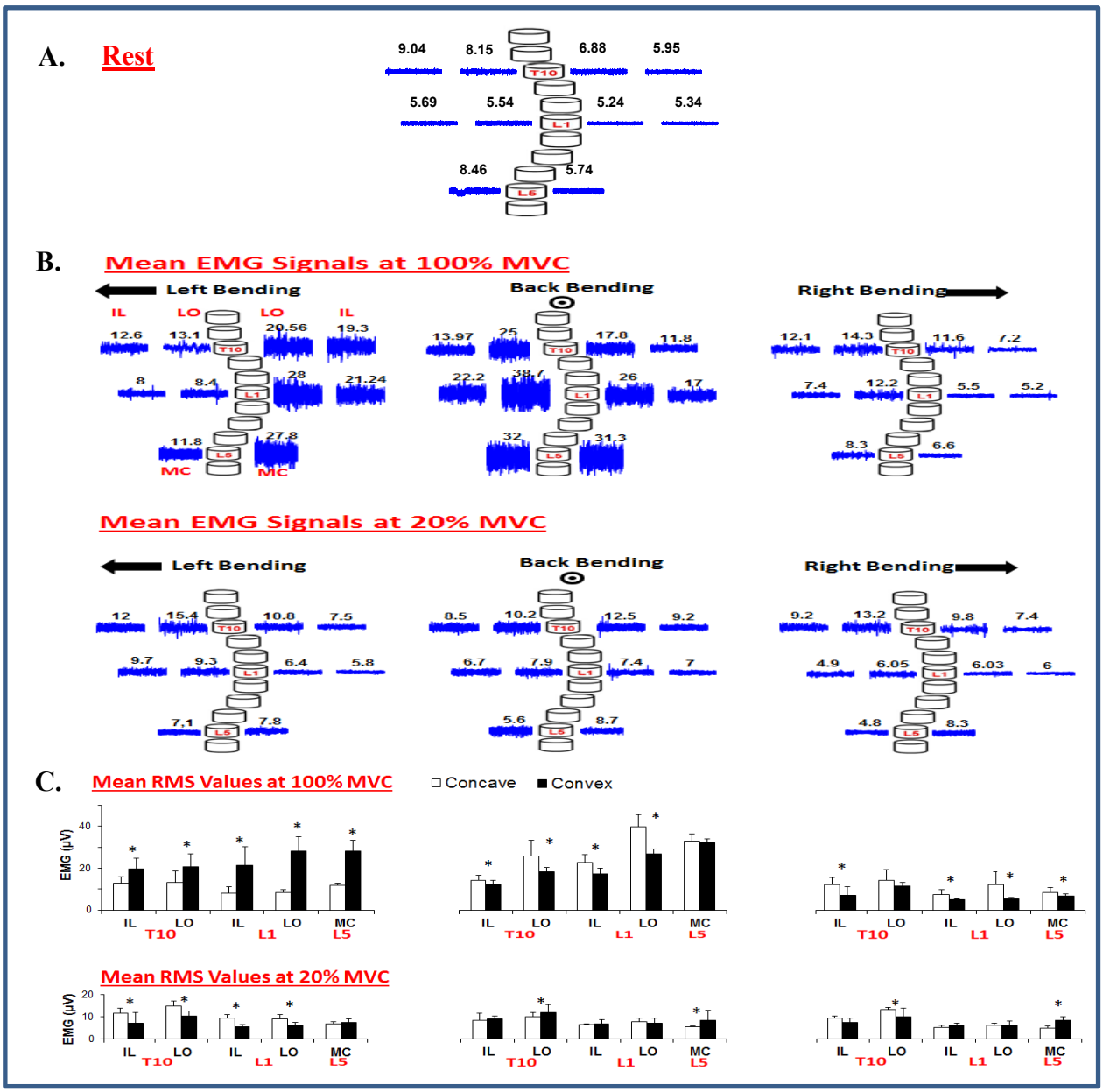

Figure 4.2 : Patient P2 (18°, R). A. EMG signals obtained at rest position**. B.** Mean EMG signals obtained from 3 trials of 5 s isometric contractions realized at 100% and 20% MVC while resisting to a pull to the right (Left Bending), a front pull (Back Bending) and a pull to the left (right Bending). Recording were made at the T10, L1 and L5 levels with the iliocostalis activity recorded at 6 cm from the spine and the longissimus activity at 3 cm from the spine. At L5, activity is from the common mass at 3 cm from the spine. **C.** means (± SD) obtained from 30 RMS values calculated on 10 contiguous 0.5 s section obtained from each set of 3 trials. Results are in black for the convex side and in white for the concave one. *p< 0.05 significance level (Student t-test).

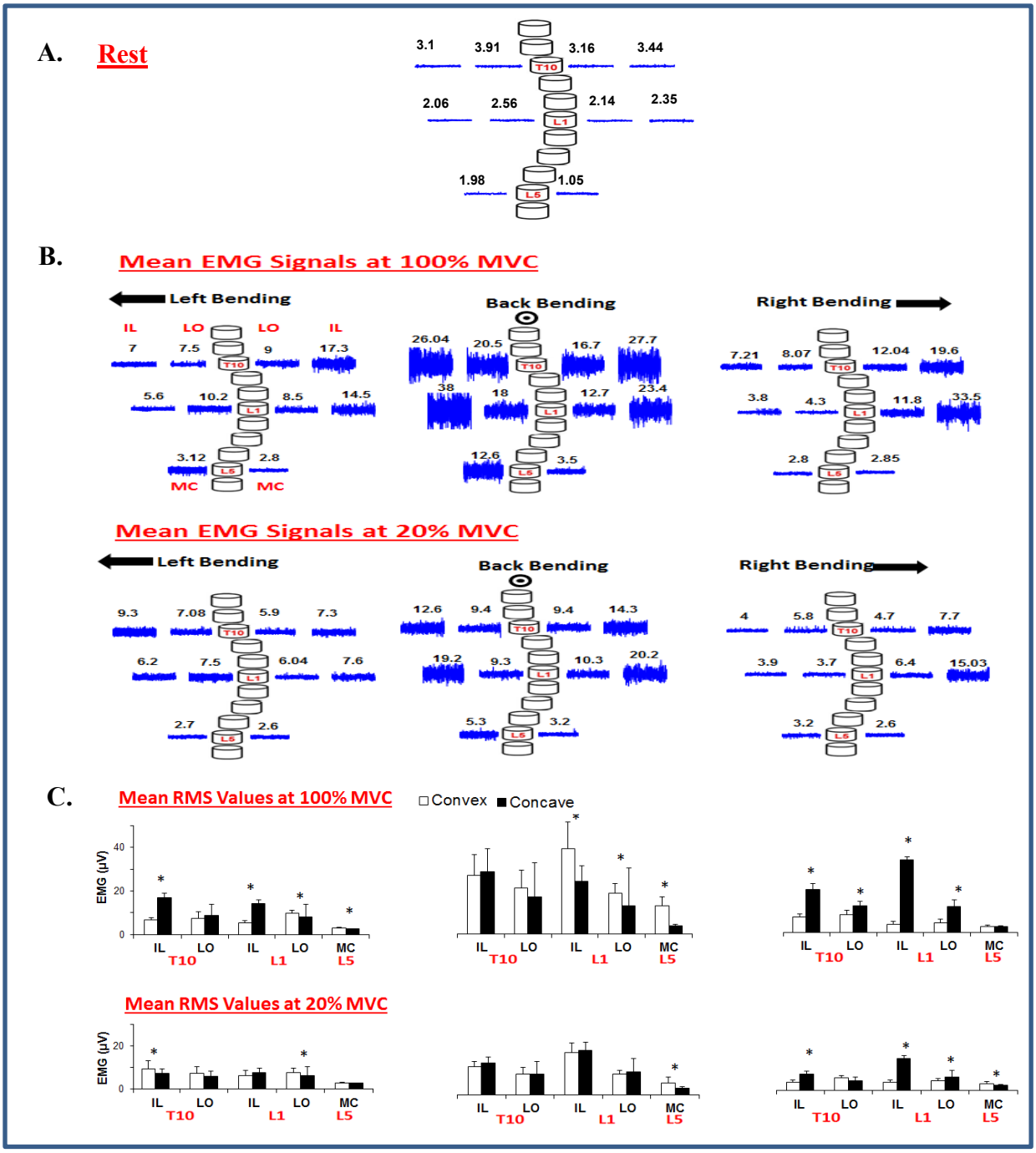

Figure 4.3: Patient P3 (30°, R). A. EMG signals obtained at rest position**. B:** Mean EMG signals obtained from 3 trials of 5 s isometric contractions realized at 100% and 20% MVC while resisting to a pull to the right (Left Bending), a front pull (Back Bending) and a pull to the left (right Bending). Recording were made at the T10, L1 and L5 levels with the iliocostalis activity recorded at 6 cm from the spine and the longissimus activity at 3 cm from the spine. At L5, activity is from the common mass at 3 cm from the spine. **C:** means (± SD) obtained from 30 RMS values calculated on 10 contiguous 0.5 s section obtained from each set of 3 trials. Results are in black for the convex side and in white for the concave one. *p< 0.05 significance level (Student t-test).

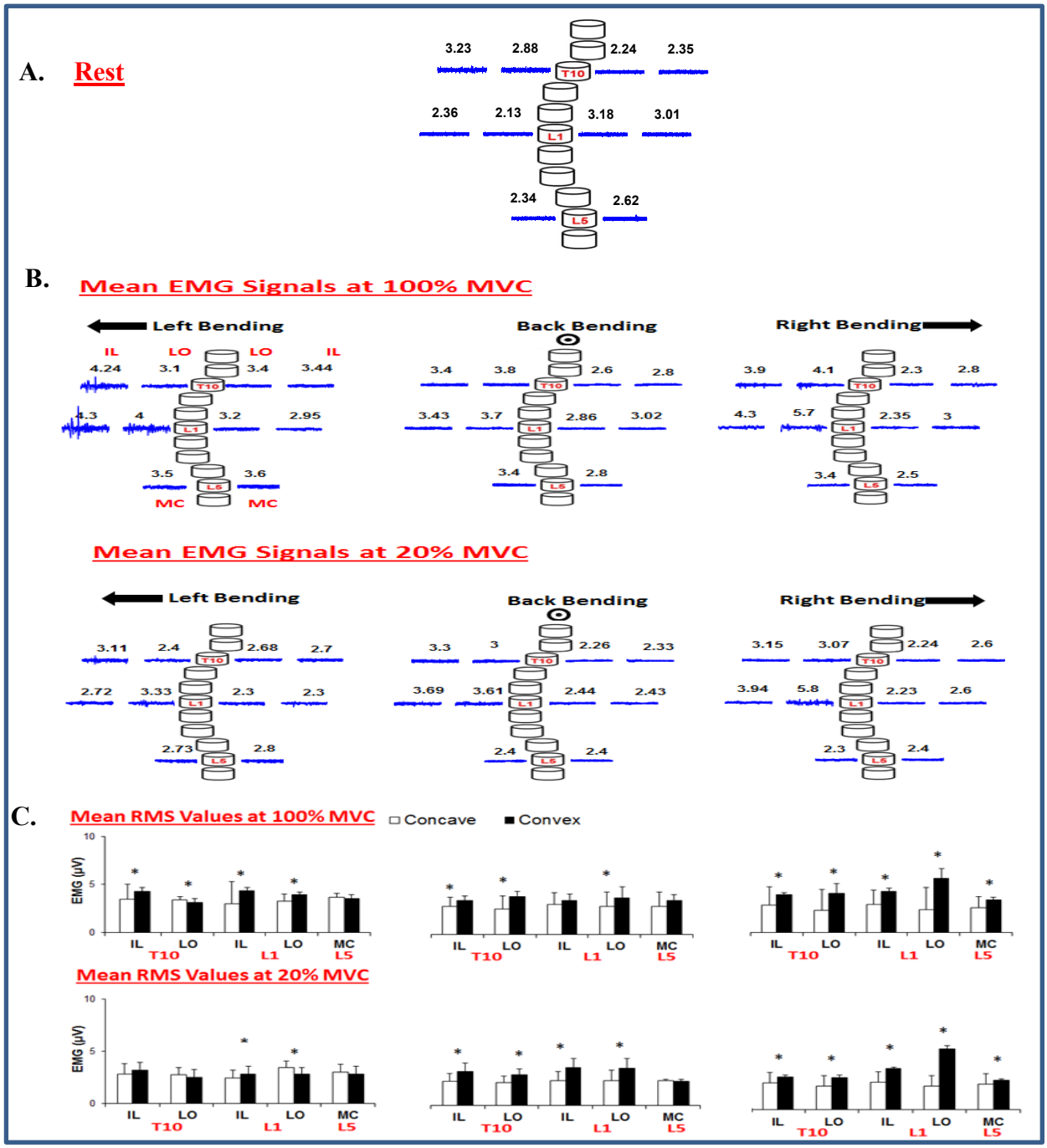

Figure 4.4: Patient P4 (32°, L). A. EMG signals obtained at rest position **B.** Mean EMG signals obtained from 3 trials of 5 s isometric contractions realized at 100% and 20% MVC while resisting to a pull to the right (Left Bending), a front pull (Back Bending) and a pull to the left (right Bending). Recording were made at the T10, L1 and L5 levels with the iliocostalis activity recorded at 6 cm from the spine and the longissimus activity at 3 cm from the spine. At L5, activity is from the common mass at 3 cm from the spine. **C.** means (± SD) obtained from 30 RMS values calculated on 10 contiguous 0.5 s section obtained from each set of 3 trials. Results are in black for the convex side and in white for the concave one. *p< 0.05 significance level (Student t-test).

To summarize the differences between the paraspinal activities of our patients, the previous results at 100% MVC have been regrouped in Fig. 4.5. As can be seen for the Back Bending task where those differences are best observed, larger EMG signals on the concave side are present for the first three patients for whom a progression of their spinal deviation could be expected. As for P4, more activity on the convex side could indicate a possible reduction of his scoliosis.

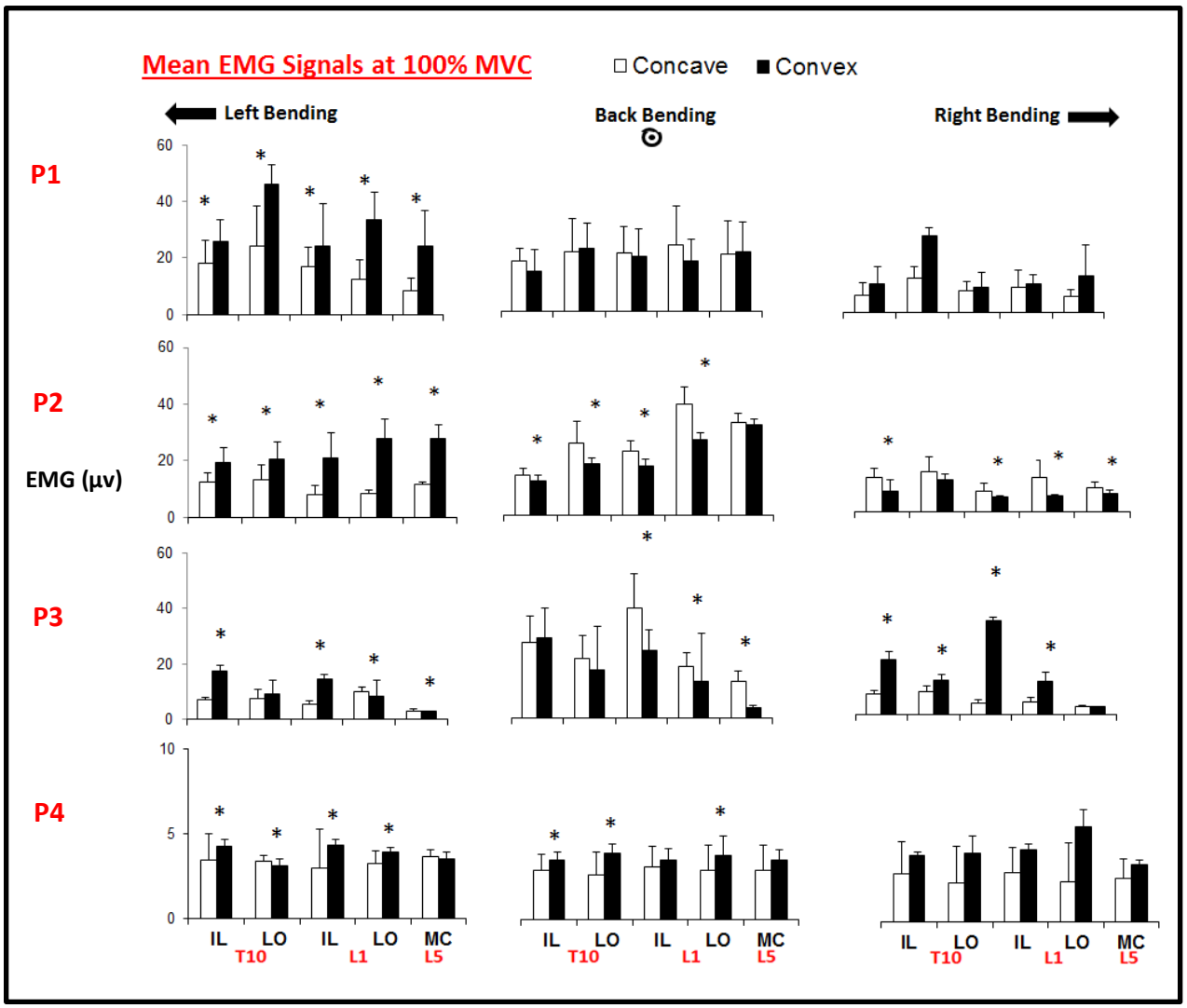

Figure 4.5 : Mean (± SD) EMG signals obtained from 3 trials of 5 s isometric contractions realized at 100% MVC for P1, P2, P3 and P4 while resisting to a pull to the right (Left Bending), a front pull (Back Bending) and a pull to the left (Right Bending). Recording were made at the T10, L1 and L5 levels with the iliocostalis activity recorded at 6 cm from the spine and the longissimus activity at 3 cm from the spine. At L5, activity is from the common mass at 3 cm from the spine. Results obtained from 30 RMS values calculated on 10 contiguous 0.5 s section obtained from each set of 3 trials. Results are in black for the convex side and in white for the concave one. *p< 0.05 significance level (Student t-test).

Controls. Four healthy adolescent boys were enrolled in the experimental protocol as a control group. EMG levels between right and left ES muscles didn't demonstrate any significant difference during back bending. As expected, for each of the 4 controls, significant higher EMG activity was present on the left side during the left bending task and the opposite during the right bending task. An example of the EMG results obtained from C2 during the 3 trunk bending tasks is shown in Fig 4.6.

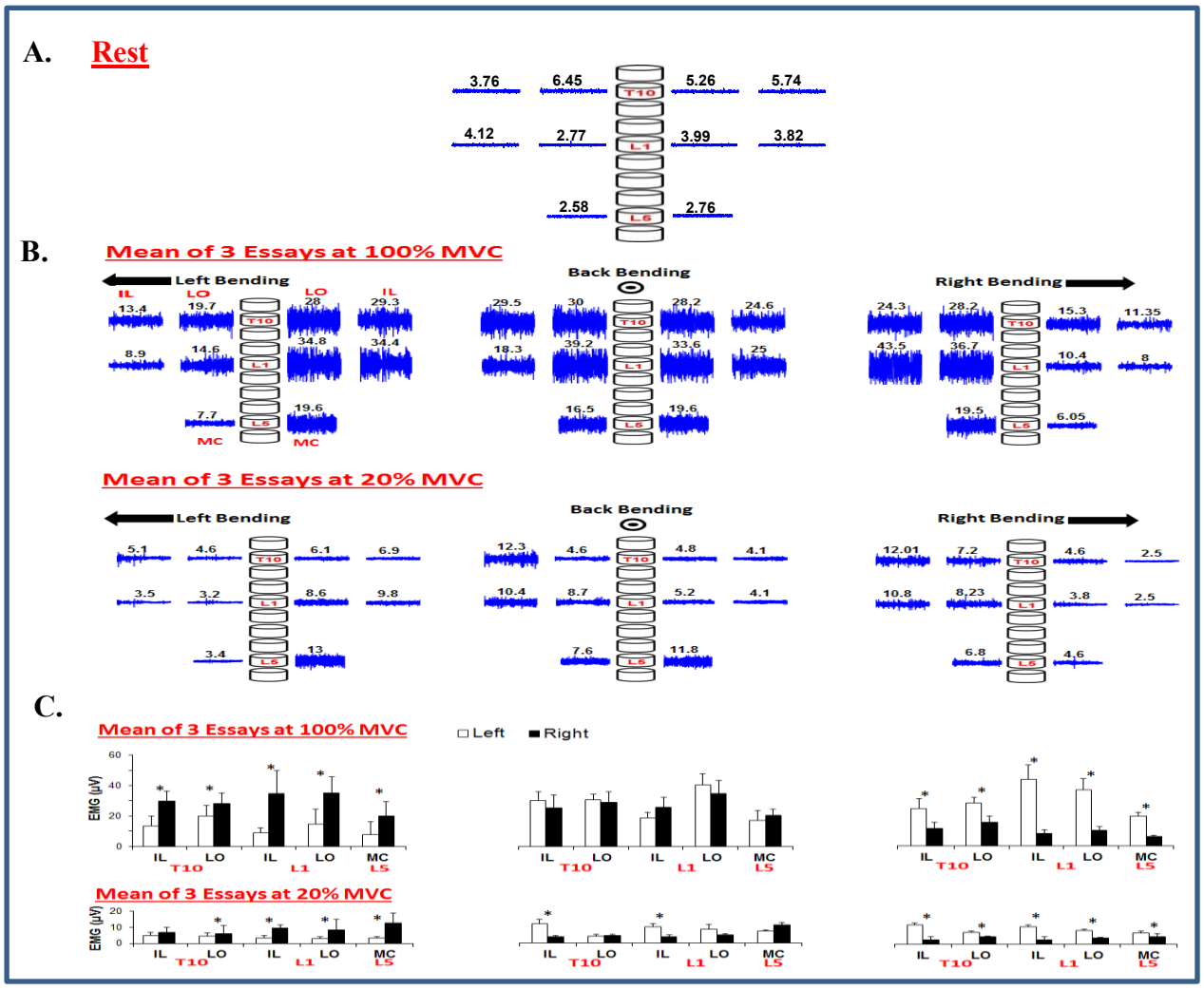

Figure 4.6: Control C2. A. EMG signals obtained at rest position **B.** Mean EMG signals obtained from 3 trials of 5 s isometric contractions realized at 100% and 20% MVC while resisting to a pull to the left (Right Bending), a front pull (Back Bending) and a pull to the right (Left Bending). Recording were made at the T10, L1 and L5 levels with the iliocostalis activity recorded at 6 cm from the spine and the longissimus activity at 3 cm from the spine. At L5, activity is from the common mass at 3 cm from the spine. **C.** means (± SD) obtained from 30 RMS values calculated on 10 contiguous 0.5 s section obtained from each set of 3 trials. Results are in black for the convex side and in white for the concave one. *p< 0.05 significance level (Student t-test).

To get a general view of the muscular activity on both sides of the spine, the 5 mean results obtained on one side of the spine were grouped together and compared to what happened on the other side. As shown in Fig. 4.7 for the back bending task at 100% MVC, for each control subjects and FA patients, a significant difference was only detected once among the controls while three significantly differences were found among the FA patients: twice on the concave side for two of them and on the convex side for P4.

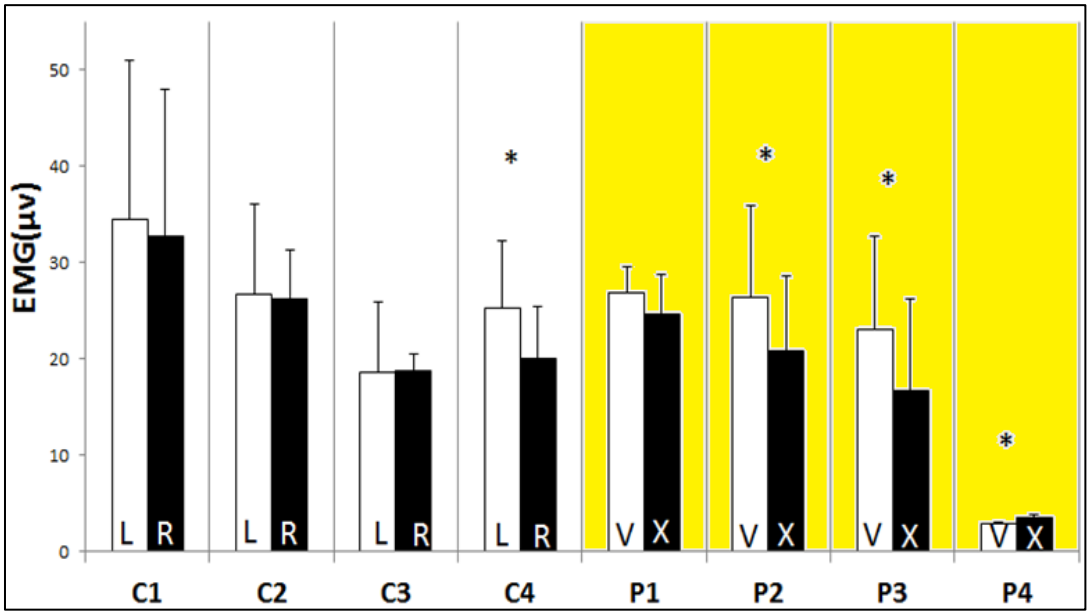

Figure 4.5: Mean (+standard deviation) RMS values of the 5 signals collected at the both sides of the spine obtained from the 4 control subjects and 4 FA patients during the back bending task at 100 % MVC (X: Convex, V: Concave, L:left, R: right). * Anova test with $p < 0.05$.

4.2 Ultrasound Results

In Fig. 4.8, US images from the convex and concave back muscles of P2 are presented. Over those images, the spinous process (SP) and the visually estimated contour of the ES muscle were drawn in order to obtain its cross-section area (CSA). Distance from the top of each image up to the upper limit of the ES was taken as an indication of the skinfold thickness. Increasing quantities of subcutaneous fat tissue reduces the relative differences in the distances between the muscle fibers of interest and the electrodes located above the different muscles, causing the action potentials to appear more similar at each electrode and resulting in a decrease in surface EMG amplitude.

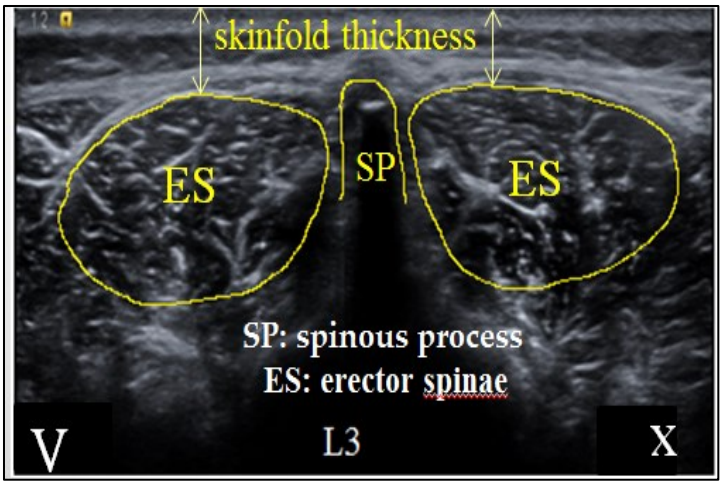

Figure 4.6: P2 back muscles US images at L3 level for the concave (left) and convex (right) side. Yellow lines outline the contour of the ES (Erector Spinae) and of the spinous process (SP). The arrowed lines on top are to estimate the skinfold thickness on each side of the spine.

On the US images over L4 to T8 (where apex of the scoliotic curvature is usually located) a manual segmentation with StradWin (v4.6) software was done on the ES muscle on both sides of the spine for determining their volume. At each vertebral level, depending on the probe's speed during a scan, segmentation was done from 10 to 14 slices out of the recorded ones i.e. ~100. C2 and P1 results are presented in Fig. 4.9

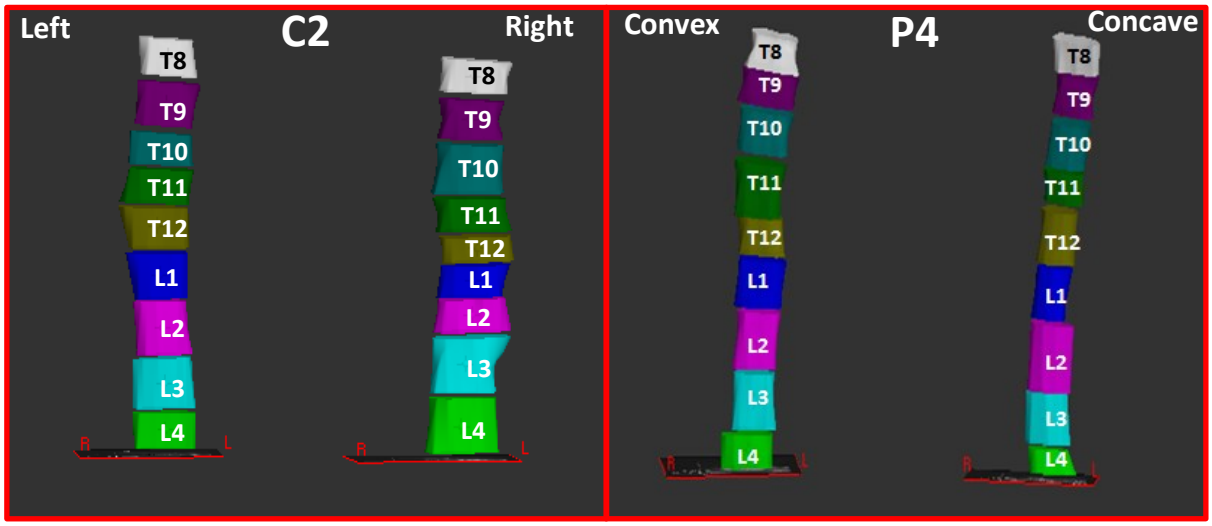

Figure 4.7: StradWin screenshot 2D reconstitution of the ES muscles between T8 and L4 on both sides of the spine for C2 and P4

As presented in Table 1, between T8 to L4, the volume of the ES muscle ranged from 29 to 97 cm^3 for the patients depending on the physical condition and the age of the patients. Volumes of the control subjects where larger.

Table 4.1: Erector spinae muscles volume (cm^3) for 4 FA patients and 4 controls measured between T8 and L4

FA Patients	Concave	Convex
P1	29 ±0.9	37 ±1.6
P2	74 ±1.3	73 ±1.1
P3	40 ±1.3	97 ± 1.2
P4	61 ±1.8	59 ±0.9
Controls	**Left**	**Right**
C1	117 ±2.4	112 ±2.7
C2	64 ±1.3	66 ±1.5
C3	68 ±2.4	73 ± 2.8
C4	120 ±1	119 ±1.3

For P1 and P3 with a right scoliosis (Cobb angle of 40° and 32° respectively), the ES muscle volume was larger on the convex side at most levels as shown in Fig 4.10 A. For P1, the muscular volume between T8 and L5 on the convex side was higher than on the convex one. For P3, the difference was appreciably large between the two sides and this is associated to an important difference of volume at the apex of the deviation. For P2 at the thoracic level, the ES volume was larger on the concave side (41.4 vs 38.0 cm^3) than on the convex one while at the lumbar level it was the opposite. From T8 to L4 practically no volume difference was detected between the concave side and the convex one. For P4 with a left scoliosis, a slight difference was detected between the concave and the convex side.

The skinfold thickness ranged between 40 to 82 mm. The CDI index for the differences in CSA was calculated for the 4 patients and shown in Fig. 4.10B, where the blue bars indicated the levels along the spine where concave CSA is higher than on the convex side and the red bars

indicates the opposite where convex CSA is higher than on the concave side along the spine. As can be seen in the figure for P1, P3 and P4, the CSA of convex was higher than the concave from L1 to T10, where the apex of the scoliosis is usually found, except for P1 at T12 level where the concave CSA was higher than the convex.

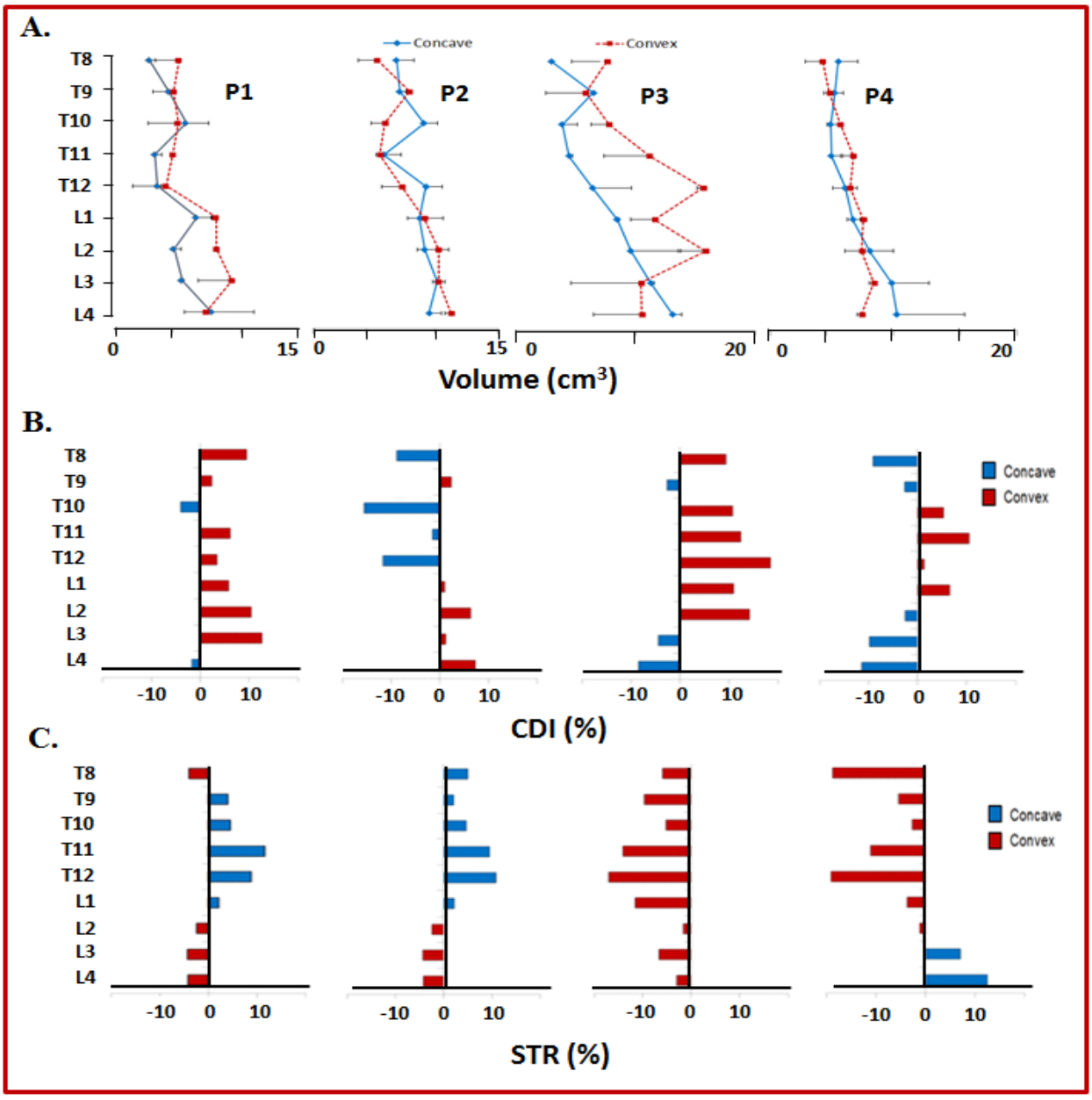

Figure 4.10: Panel A: Average (- or +SD) ES volume obtained from L4 to T8 on the concave (solid blue line) and on the convex (red dotted line) of the four patients. **Panel B:** calculated CDI index: blue bars indicate levels where the concave cross sectional area was higher than the convex one and red bars for the opposite. **Panel C:** represents the calculated STR value, blue bars indicate spinal levels with a larger skinfold thickness of the concave than the convex side and the red ones indicate the opposite.

4.3 Phase 1: Experiments with Duchenne Muscular Dystrophy

As mentioned in the Introduction, our experiments with FA patients were considered as a Phase II project relative to a previous one (i.e., Phase I realized by Thouin (2005)). Both projects had the same goal: investigate the muscular contribution to the development of scoliosis. In Phase I, data where obtained from 10 DMD patients: 5 were classified as non-scoliotic (NS), 3 as pre-scoliotic (PS) since they only had a slight spinal deviation (Cobb angle < 15°) and 2 were clinically classified as scoliotic (S). It was found that EMG activity was similar on both sides of the spine for the NS patients as with the five healthy control subjects. As for the PS patients, higher activity was found on the concave side while for the two S patients, one had a significant ($p<0.01$) higher muscular activity on the convex side than on the other side. No significant difference was found for the other S patient probably due to her low EMG levels associated to weak contractions and a large subcutaneous fat layer as indicated by an elevated BMI. Approximately one year after the first data acquisition, many of those 10 patients came back in the laboratory for a follow-up. The same EMG experimental protocol was used but the data of three of them were not analyzed. We; we extended our analysis to those data.

4.3.1 Comparison between visits 1 and 2

With a separation of 12 to 17 months between the 2 visits, it was interesting to see how the spine condition of the three patients evolved. As can be seen in Table 4.2 two non scoliotic patients at the first visit (D4 and D5) saw a deterioration of their condition as they started to develop a scoliosis. In contrast, D6 saw a complete regression of his 8° scoliotic deformation. For comparison purposes, results of these three patients are presented side by side in figures 4.11, 4.12 and 4.13.

Table 4.2: Some characteristics of our 3 DMD patients

Patients	Age (years)	Weight (kg)	Height(cm)	BMI(kg/m^2)	Cobb angle (apex position)	Classifications	Visit#1	Visit #2	Delay (month)
D4	10.0	29.6	130	18	0	**NS** (Non-Scoliotic)	NS	PS 7° (T12,L)	12
D5	12.5	32.3	123	21	0		NS	PS 8°(T6,R) 10° (L3,L)	12
D6	13.7	35.5	129	21.3	7° (T9,R)	**PS** (Pre-Scoliotic)	PS	NS	16.5

In her first visit, patient D4 patient, showed a significant higher activity was observed for left longissimus dorsi and illiocostalis group at T10 level at 100 and 70% MVC during back bending task ($p<0.003$) and significant higher activity for left longissimus dorsi at L1 level at 100% for the same task. Whether he was resisting to a left or right pull, the mean RMS value presents the higher activity of right than left at different MVC, but this difference was only significant at 70% for both tasks. However, in her second visit (14 months later), mean RMS values had increased on both sides at different MVC, 2 times higher than his first visit. For the three tasks, a significantly greater activity on her right side at 70% MVC which corresponds to the concave side of her spine deviation was observed. Amplitudes of EMG signals obtained from D4 on two occasions are presented in Fig. 4.11.

Patient D5 did not show a scoliotic deviation at the first visit and no great difference was observed between left and right side results (Fig.4.12). In his second visit 12 months later, he had developed a double scoliotic curve: one of 8º on the right at T6 and one of 10º on the left at L3. A significantly higher left activity than right ($p<0.01$) at all recording sites at 100% MVC during back bending task was observed. However Mean RMS values showed no difference between left and right at 70% MVC for the same task. A pull to the right at 100% MVC was accompanied by larger activity on his right muscles at all recording sites and was significant only for longissimus at L1 and L5 in particular. As for a pull on the other direction, activity was higher at all levels but also on his opposite side and significant at L1 and L5.

Patient D6 had a deviation of 8° to the right with its apex at T11on his first visit (Fig. 4.13). As expected EMG activity was larger on the side opposite to the bending direction at 100% MVC while at 70% this was true only for the right bending. On back bending, activity was always larger on the convex side for the two contraction levels and at 70% MVC, those differences were all significant. During his second visit (16 months later), his spine curvature had disappeared and his muscle activity was different. Contrary to the first visit, at 100% MVC, more activity was seen on the same side of the bending. At 70% MVC, the left bending condition produces similar results as in the first visit but different ones for the right bending. For the back bending results, activity was present on its previously convex side.

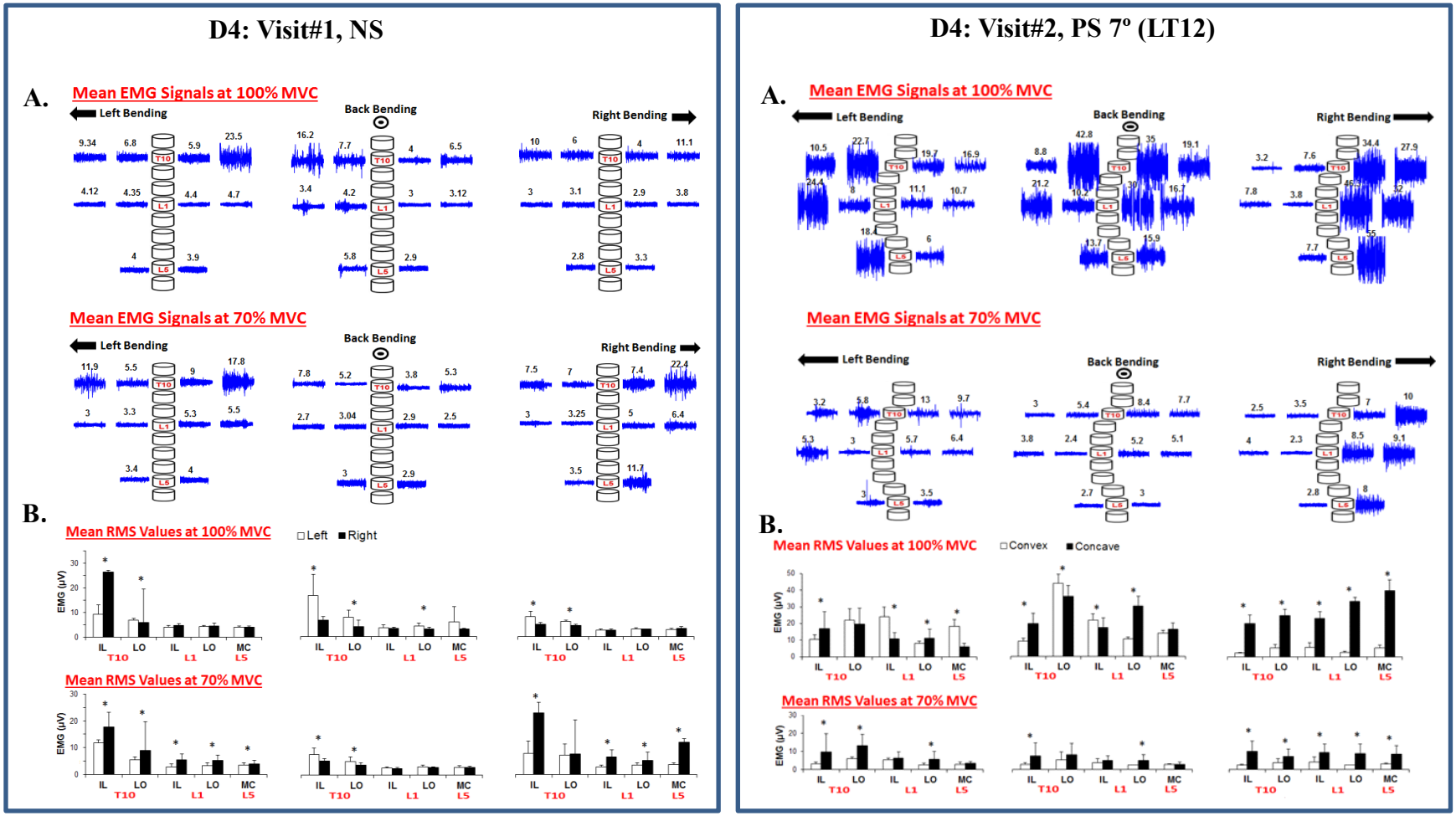

Figure 4.8: Patient D4: visit #1 & visit #2. Panel A: Mean EMG signals obtained from 3 trials of 5 s isometric **c**ontractions realized at 100% and 70% MVC while resisting to a pull to the left (Right Bending), a front pull (Back Bending) and a pull to the right (Left Bending). Recording were made at the T10, L1 and L5 levels with the iliocostalis (IL) activity recorded at 6 cm from the spine and the longissimus (LO) activity at 3 cm from the spine. At L5, activity is from the mass common (MC) at 3 cm from the spine. **Panel B:** means (± SD obtained from 30 RMS values calculated on 10 contiguous 0.5 s section obtained from each set of 3 trials. Results from the convex side are in black and in white for the concave one. *p< 0.05 significance level (Student t-test)

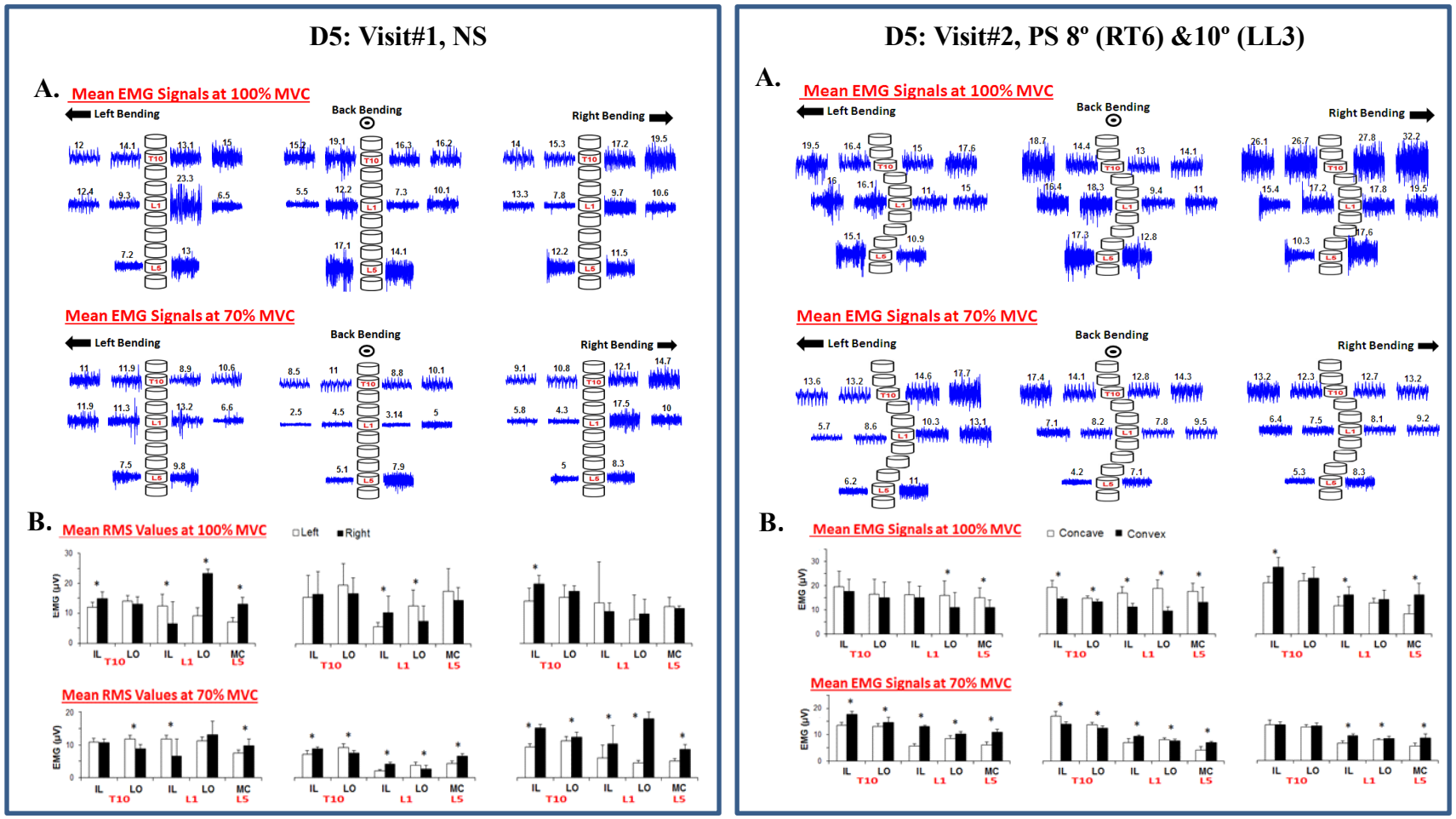

Figure 4.9: Patient D5: visit #1 & visit #2. Panel A: Mean EMG signals obtained from 3 trials of 5 s isometric **c**ontractions realized at 100% and 70% MVC while resisting to a pull to the left (Right Bending), a front pull (Back Bending) and a pull to the right (Left Bending). Recording were made at the T10, L1 and L5 levels with the iliocostalis (IL) activity recorded at 6 cm from the spine and the longissimus (LO) activity at 3 cm from the spine. At L5, activity is from the mass common (MC) at 3 cm from the spine. **Panel B:** means (± SD obtained from 30 RMS values calculated on 10 contiguous 0.5 s section obtained from each set of 3 trials. Results from the convex side are in black and in white for the concave one. *p< 0.05 significance level (Student t-test)

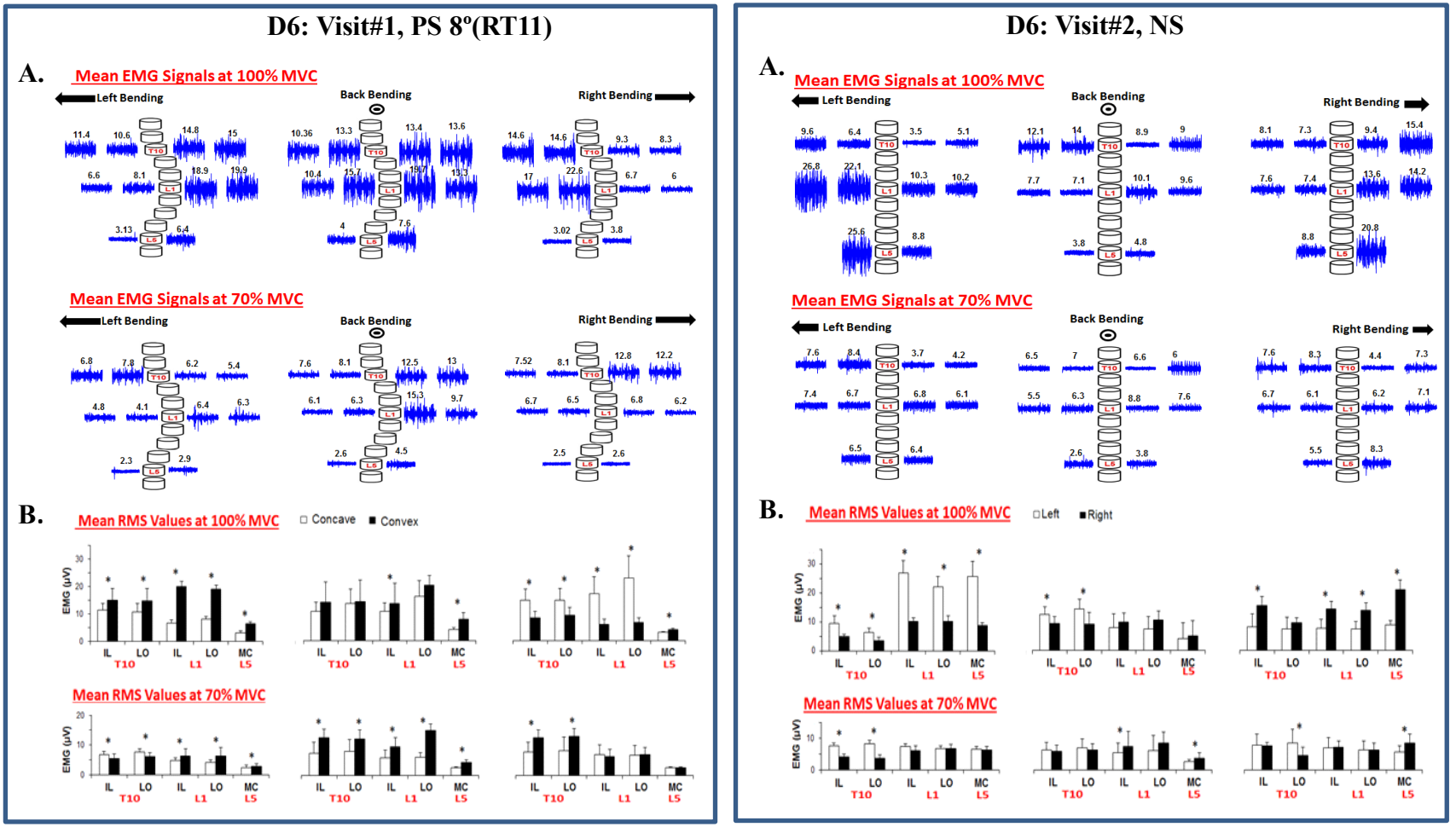

Figure 4.10 : Patient D6: visit #1& visit #2. Panel A: Mean EMG signals obtained from 3 trials of 5 s isometric **c**ontractions realized at 100% and 70% MVC while resisting to a pull to the left (Right Bending), a front pull (Back Bending) and a pull to the right (Left Bending). Recording were made at the T10, L1 and L5 levels with the iliocostalis (IL) activity recorded at 6 cm from the spine and the longissimus (LO) activity at 3 cm from the spine. At L5, activity is from the mass common (MC) at 3 cm from the spine. **Panel B:** means (± SD obtained from 30 RMS values calculated on 10 contiguous 0.5 s section obtained from each set of 3 trials. Results from the convex side are in black and in white for the concave one. *p< 0.05 significance level (Student t-test).

To facilitate the comparisons between the results obtained from our three DMD patients between their two visits, a grouping of some of the previous results are shown in Fig. 4.14.

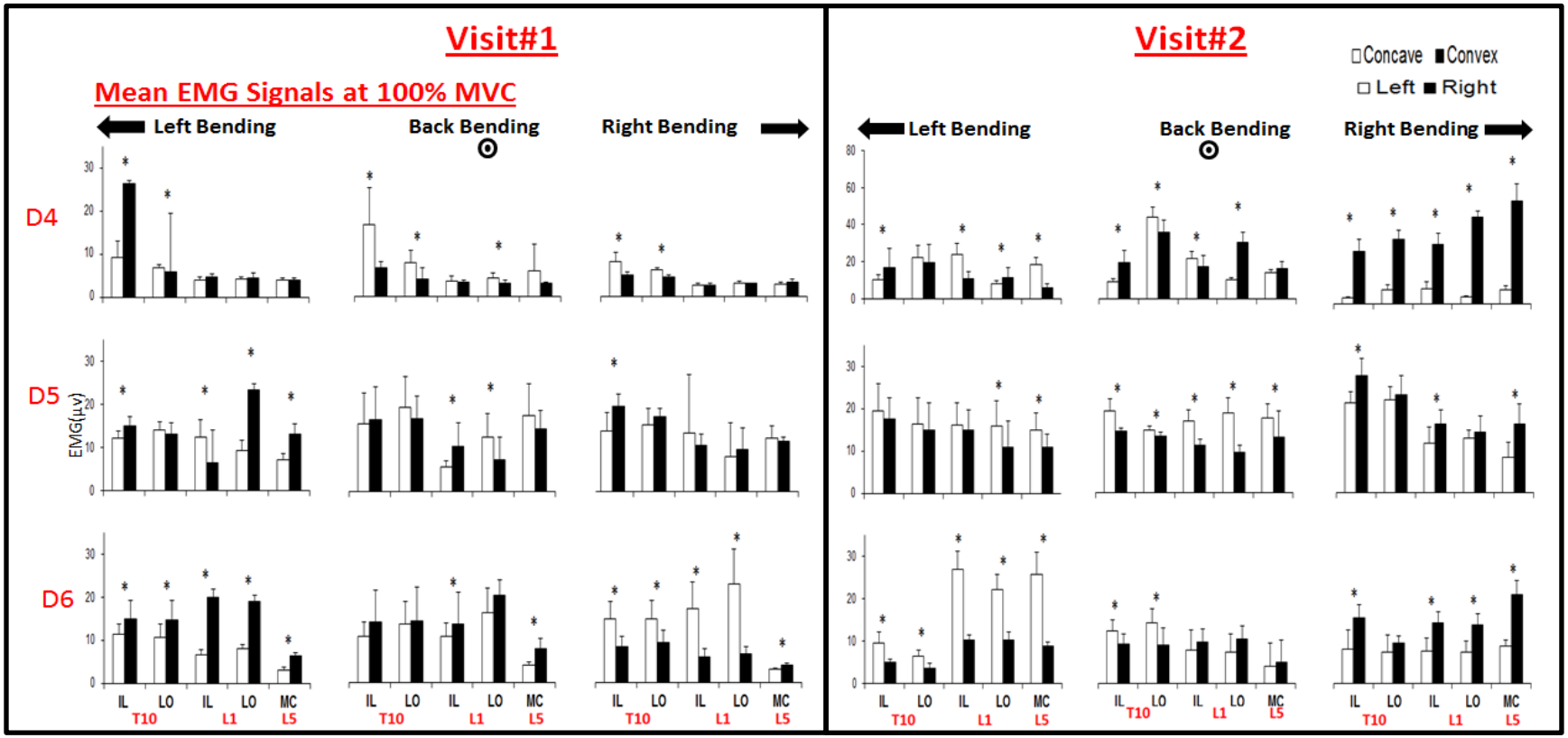

Figure 4.14 : Mean (± SD) EMG signals obtained from 3 trials of 5 s isometric contractions realized at 100% MVC for D4, D5 and D6 during visits #1 and #2 while resisting to a pull to the right (Left Bending), a front pull (Back Bending) and a pull to the left (Right Bending). Recording were made at the T10, L1 and L5 levels with the iliocostalis activity recorded at 6 cm from the spine and the longissimus activity at 3 cm from the spine. At L5, activity is from the common mass at 3 cm from the spine. Results obtained from 30 RMS values calculated on 10 contiguous 0.5 s section obtained from each set of 3 trials. Results are in black for the convex side and in white for the concave one. *p< 0.05 significance level (Student t-test).

Chapter 5: Discussion

Despite many years of research effort, the aetiology of AIS is still unknown. For many investigators (Avikainen et al., 1999; Zettergerb et al., 1983; Odermatt et al. 2004; Thouin 2005; Cheung et al., 2005), a possible causative factor in the production and progression of AIS is uneven activity of the paraspinal muscles. The predominance of convex paraspinal muscles near the curve apex and at the end-point of the curvature was reported by Reuber et al. (1983), Avikainen et al. (1999), Mooney et al. (2000) and Cheung et al. (2004).To explain those differences, differences in the muscle composition was proposed (Sahgal et al., 1983; Zetterberg al., 1983; Ford et al., 1984; Bylund et al., 1987 and Mannion et al., 1998). Others believed that the increased myoelectric activities on the convex side were only a secondary effect of the muscles adapting to a higher load demand in larger curves.

Many investigations have been done on AIS patients, few on DMD ones and, to our knowledge, none on FA patients prior to ours. Our objective was to study the paraspinal muscles activity along and on each side of the spine of FA patients. To facilitate the interpretation of the collected EMG signals, the volume of those muscles on each side of the spine and their distance from the skin surface was obtained. To do so, the same experimental protocol used in a previous project with DMD was repeated with the FA patients and US images was used to replace the MRI ones.

During the three different bending tasks, significant alterations in muscle activity were found in our group of FA patients. During back bending, EMG activity on the concave side was higher than on the convex one for the three right scoliotic patients P1, P2 and P3. At the opposite, amplitude of the EMG signals of P4 was greater on his convex side. During left bending (resisting to a right pull) at 100% MVC, activity on the opposite side was higher as expected for P1 and P3 but, unexpectedly, for P2 at all recording sites the inverse was found. At 20% MVC left bending, higher activity was found on the concave side for P2 and P3, and for P1, this was the opposite.

When five mean results obtained on one side of the spine were grouped together and compared to what happened on the other side for the back bending task at 100% MVC (Fig.

4.7), for each control subjects and FA patients, a significant difference was detected once among the controls while three significantly differences were found among the FA patients: twice on the concave side for two of them and on the convex side for P4. Such results indicated that while C4 showed a muscular imbalance, considering that at 13 years old and measuring 174 cm, his growth spur could be mainly over, he has a minimal risk of developing a scoliosis. As for P1, P2 and P3, a larger muscular activity was detected (significant for P2 and P3) on the concave side of their spinal deviation. This indicates that those scoliotic curves are at risk of progressing in the future. As for P4, the presence of significant higher activity on his convex side points toward a possible regression of his spinal deviation.

Every FA patient presented special complications. Although P1 was 10 years old and the youngest of the group, he had the largest degree of scoliosis (40º) but was ambulant. Activity of all his muscles was higher than that of the other patients due probably to the physical exercise program that he was following. The results of P2 with 18° curve were of the same amplitude as those of the control subjects during the left and right bending and during the back bending task, his concave activity was higher than on the convex one as in pre-scoliotic DMD patients. Patient P3 was non-ambulant and he had difficulty to maintain his balance while performing bending tasks and we had to help him to keep the position. Patient P4, with a left scoliosis of 32°, had a significantly larger paraspinal activity on the convex side of the deviation in agreement with results reported with DMD and AIS patients. At rest, before and at the end of the experiment, his EMG activity was also larger on the convex side. While this is interesting, it should be noted that the amplitude of all his signals was appreciably less than that of the other FA patients. This was partly due to a skinfold thickness of 12 mm, compared to ~7 mm for the three others patients and to an important muscle weakness.

The spine stability depends on the interaction of intrinsic factors (vertebrae, facet joints, ligaments) with extrinsic factors such as gravity and muscular forces. Our AF patients had a

moderate scoliotic deviation (18° to 40°) but during the experiments their ability to maintain a stable sitting position was not very good which is different from what was observed with the DMD patients studied by Thouin (2005). In absence of information on the intrinsic factors of FA and DMD patients, it would seems that while sharing some similitude in their back muscle activity, scoliotic FA patients muscle impairment would be more important than for the DMD patients.

Mooney et al. (2000) suggested that asymmetrical spinal muscle activation may not be caused by the curvature itself but may have its origin in the central nervous system. In 1982, Mixon and Steel proposed that altered cerebral/subcortical function or hemispherical dominance could be related to AIS. Burwell et al. (2009) suggested that alteration of the motor drive in the spinal cord, either from altered sensory input or from a central mechanism, may produce enough lateral deviation and axial rotation to disturb the delicate balance of forces thereby producing AIS. If this also applies to the asymmetrical spinal muscle activation in our FA patients, it seems that areas of the nervous system involved in maintaining an upright posture is also altered.

Considering the volume of the ES muscle and the skinfold thickness under the surface covered by our electrodes, for right scoliotic patients, P1 and P3, nearly at all level, a larger ES volume was detected on the convex side of the deviation. The same results were found for P2 at lumbar region, while the opposite was detected at the thoracic region. For the left scoliotic patient P4, the volume on the concave side was only larger at T8 and between L2 to L4 levels. The skinfold thickness, at most vertebral levels, was larger on the concave side for P1 and P2 and on the convex one for the two other patients (P3 & P4). We found that the volume and skinfold thickness could be higher either on the concave side or the convex side. Those results are quite similar to those of Zoabli et al. (2004) who analyzed the magnetic resonance images (MRI) of 88 AIS patients and found that a larger muscle volume could either be found on the convex or concave side along the spine and at the apex of the curve and a larger skinfold thickness was always found on the concave side of a

curve, especially at the apex region. They reported that rotation of the spine contributes to put uneven stretch on muscles and on the skinfold thickness thus contributing to differences in EMG level measured on the convex and concave side. When computed tomography (CT) images were used, Saka (1987), Stern and Clark (1988) and Wood (1996) all reported also a larger muscle volume on the convex side at the curve apex and the replacement of muscle tissue by fat was also found greater on the concave side.

Scoliosis being a 3D deformation, in addition to the frontal deviation where the Cobb angle is measured, there is also a rotation of the spine along its vertical axis. This results in an elongation and stretching of the muscles on the convex side and a muscle length shortening on the concave side which induce a larger CSA than on the convex side (Kim et al., 2013). With our FA patients, we found that a larger volume (thus CSA) of the ES muscles could be on either the concave or the convex side. It thus seems that for some of our patients there could have been an atrophy of their paraspinal muscles on the concave side or a hypertrophy on the convex one for P1, P3 and P4 and the opposite for P2. So, in an effort to maintain their balance, these persons were expected to display higher EMG signals over atrophied muscle and smaller signals over hypertrophied ones. But the opposite was found: higher EMG signals were detected from muscles that could have been hypertrophied. This could be associated to the fat infiltration factor which was unfortunately not possible to measure in the US images, since unlike MRI, it does not provide reliable measurement of degenerative changes in muscle such as fatty infiltration and atrophy (Whittaker et al., 2007). So, further experimental work with FA patients and more in-depth US image analysis are needed to resolve that problem.

As it is known by health care providers taking care of scoliotic persons, some curves progress over time, but not all of them while for some lucky ones, the deformation gets smaller and even disappears. This was observed between the first visit and the second one a year later. For the three patients concerned in the present study, while D4 and D5 were initially non-scoliotic, a year later they had started to develop a scoliosis. In the first visit of

D4, D5 and D6, a muscle imbalance at T10 and L1 levels was present and this situation could be at the origin of the onset of their spine deformation. Being 10 and 12.5 years old, this imbalance factor was acting during a critical period associated to the rapid adolescent skeletal growth as is known for AIS. More luckily, D6 (13.7 years old) who was pre-scoliotic (7° at T9) at the first visit had a complete disappearance of his spinal deviation 16.5 months later. This patient displayed in his first visit a significantly larger EMG activity on the convex side from T10 to L1. In his case, the direction of the resulting net force was counteracting his spinal deviation and with time, seems to have successfully contributed to its disappearance.

During the Thouin project in 2005, all DMD patients were taking Deflazacort, a corticoid which could slow the puberty growth. Although their Cobb angle was less than 18º, all of them were using a wheelchair. For our FA group, none of them were taking medication, P1 and P2 with a deformation of 40º and 18º, both were ambulant, while P3 and P4 (30° & 32°) were wheelchair-dependent. The difference for the ambulant/wheelchair condition between FA and DMD patients could be connected to the larger paraspinal EMG signals produced by FA patients than for the DMD ones. Commonly, the progressive muscle wasting and the need for wheelchair starts at about 9 to 11 years of age for DMD patients (Kinali et al. 2008), while for FA patients, they become confined to a wheelchair 12 to 15 years after the appearance of their symptoms (Geoffroy et al. 1976). For our P1, P2, P3 patients, the trunk muscles level on both sides of the spine was almost at the same level of our controls (P4 was an exception due partly to his important skinfold thickness). Paraspinal muscle impairment thus occurs latter in FA than in DMD patients. In FA, the need for a wheelchair would be associated to a difficulty in controlling balance and movement but not to muscle strength which appears to be quite intact.

Considering that our 3 right FA patients produced more EMG signal on the concave side of their spinal deviation which is a situation also found in pre-scoliotic DMD patients, their spinal deformation will probably progress even if their Cobb angles is quite important. At

the opposite, for P4 with left scoliosis, one may see an improvement in his condition due to larger EMG signals on the convex side. This is supported by DMD patient's results, when a higher activity was present on the convex side of a scoliotic curve at the first visit; the deviation had regressed one year later. However, if an EMG imbalance was observed in a non scoliotic patient, a deviation was detected later. So, for those patients, a frequent medical follow-up is important for measuring the progression of their spinal deviation. If a second visit to the lab is possible it would be very interesting to verify if the spinal deformation progressed as it was done with DMD patients.

Chapter 6: Conclusion

Knowledge on abnormal spinal structures has been around for centuries but the scoliosis pathology still remains poorly understood. Among many of the factors involved, we focused on the muscular factor, i.e., an uneven activity of the back muscles which are lying on each side of the spine. Our hypothesis at the effect that similar EMG activity would be displayed by both DMD and FA patients was verified. However since the ability of our AF patients to maintain a stable sitting position was not as good as the one of DMD patients, it would appear that the muscular impairment in the Friedrich ataxia is different for the one of the Duchenne dystrophy. However, since the EMG and US measures where made only on 4 FA patients with various Cobb angles, results presented here should only be considered as cases study.

As a replacement to magnetic resonance imaging, we explored the use of US equipment coupled with a tracking system device to measure the volume of the paraspinal muscles and the skinfold thickness under the EMG electrodes. The volume of the paraspinal muscles was difficult to determine with precision because the angle of view of the probe was too small in some occasions to display all the muscles and the contours were sometimes difficult to determine with certainty. Also a pressure had to be applied to the probe to get an image, which resulted in an underevaluation of the skinfold thickness. Unless new approaches could be devised to prevent those flaws, the use of MRI is a better choice.

Although the study covers only a small number of FA patients, the presence of larger EMG signals on the concave side of a spinal deformation with FA patients is similar to pre-scoliotic DMD patients for whom the deformation is in its initial stage. It thus seems that our FA patients with more EMG activity on their concave side could see progression of their spinal deformation in the coming months in spite of their already important Cobb angle. To get information on those aspects, further experimental work with patients prone to develop a scoliosis is required.

Limitations and Perspectives

The small number of our enrolled patients is the main limitation of the project. Our goal was to have 15 patients at minimum but this was impossible to achieve in spite of many recruitment efforts and because of the small population, 1 over 50,000 people worldwide, of those patients. Even an increase from $75 to $125 (initially that increase appeared quite large by the Ethics committee standards and justification had to be given) to compensate for the time spends in the lab was not fruitful. The difficulty can be related to the situation of the parents who are overloaded by the responsibilities associated to the illness of their child. Also, the patients may be already participating in other research projects specially those where a procedure such as genetic modification of muscle proteins or a new medicament that could rapidly improve their condition. To extend the scope of the project with FA or DMD patients, new strategies have to be considered otherwise other kinds of projects have to be considered as with animals of even some fishes.

Another limitation is in the tested muscles. We only recorded ES muscles activity because its activity could be recorded at the skin surface but other trunk muscles like the psoas and quadratus lumborum are also involved in the balance of spinal column but being in a less superficial position, indwelling electrodes would be required to record their activity.

On US images, delimitation of the ES muscles contours was not easy to differentiate while skinfold measurement was not independent of the pressure applied on the probe during the scanning. It is thus difficult to link muscle volume and skinfold thickness to the observed EMG recorded levels. Another limitation is related to the use of CSA. It may not represent the physiologic cross-sectional area (pCSA) which is more closely related to the force that a muscle could produce. Obtaining that information with the US equipment would be lengthy requiring that each patient spent more time in the lab which we tried to keep as short as possible considering their physical condition. In addition with MRI also, pCSA would be difficult to obtain. CSA images are thus acceptable to obtain muscular volume.

Finally, fatty infiltration which is a replacement material following the destruction of muscle fibers, contribute to a force reduction while the muscle volume remains the same. On our US images, with the pressure applied to the probe to make contact with the skin, we could not evaluate fat thickness. For the time being this information appears to be only obtainable with the contactless MRI. So, in future data acquisitions involving DMD and AF patients, MRI modality has to be considered.

References

[1] http://www.tweedcoastchiropractic.com.au/OurServices/Chiropractic/Scoliosis.aspx. Consulted on (20-01-2014)

[2] http://mi.eng.cam.ac.uk/~rwp/stradwin/docs/calibrate.htm. Consulted on (20-01-2014)

Agur A & Dalley AF, 2008. Grant's Atlas of Anatomy. 12th Edition, Lippincott Williams & Wilkins.

Alper G & NarayananV, 2003. Friedreich's ataxia. *Pediatr Neurol,* 28, 335–341

Allard P, Duhaime M, Raso JV, Thiry PS, Drouin G & Geoffroy G. 1980. Pathomechanics and management of scoliosis in Friedreich ataxia patients: preliminary report. *Can J Neurol Sci.*, 7, 383–388

Allard P, Dansereau J, Thiry PS, Geoffroy G, Raso JV & Duhaime M. 1982. Scoliosis in Friedreich's ataxia. *Can J Neurol Sci.*, 9,105–111

Allard P, Dansereau J, Duhaime M & Geoffroy G. 1984. Scoliosis assessment in Friedreich's ataxia by means of intrinsic parameters. *Can J Neurol Sci*. 11, 582–587

Aronsson DD, Stokes IA, Ronchetti PJ & Labelle HB. 1994. Comparison of curve shape between children with cerebral palsy, Friedreich's ataxia, and adolescent idiopathic scoliosis. Dev Med Child Neurol. , 36(5), 412-8

Avikainen VJ, Rezasoltani A & Kauhanen HA. 1999. Asymmetry of paraspinal EMG-time characteristics in idiopathic scoliosis. *Journal of Spinal Disorders & Techniques*, *12*(1), 61-67

Basmajian J & De Luca CJ, 1985. Muscles Alive: Their Function Revealed by Electromyography, 5th Edition. Williams & Wilkins

Bassani E, Candotti CT, Pasini M, Melo M & La Torre M. 2008. Assessment of neuromuscular activation in individuals with scoliosis using surface electromyography. *Revista Brasileira de Fisioterapia*, 12(1), 13-19

Bogdanovich S, Perkins KJ, Krag T & Khurana TS. 2004. Therapeutics for Duchenne muscular dystrophy: current approaches and future directions. *Journal of Molecular Medicine*, 82(2), 102-115

Bowen RC, Seliktar R, Rahman T et al. 2001. Surface EMG and motor control of the upper extremity in muscular dystrophy: a pilot study. *Engineering in Medicine and Biology Society, Proceedings of the 23rd Annual International Conference of the IEEE*, 2, 1220-1223

Brockmann K, Becker P, Schreiber G, Neubert K, Brunner E & Bonnemann C. 2007. Sensitivity and specificity of qualitative muscle ultrasound in assessment of suspected neuromuscular disease in childhood. *Neuromuscular Disorders*, 17(7), 517-523

Burwell RG, Aujla RK, Grevitt MP, Dangerfield PH, Moulton A, Randell TL & Anderson SI. 2009. Pathogenesis of adolescent idiopathic scoliosis in girls - a double neuroosseous theory involving disharmony between two nervous systems, somatic and autonomic expressed in the spine and trunk: possible dependency on sympathetic nervous system and hormones with implications for medical therapy. *Scoliosis,* 31, 4-24

Butterworth TR Jr & James C, 1969. Electromyographic studies in idiopathic scoliosis. *Southern Medical Journal*, 62(8), 1008

Bylund P, Jansson E, Dahlberg E & Eriksson E. 1987. Muscle Fiber Types in Thoracic Erector Spinae Muscles Fiber Types in Idiopathic and Other Forms of Scoliosis. *Clinical orthopaedics and related research*, 214, 222

Cady RB & Bobechko WP, 1984. Incidence, natural history, and treatment of scoliosis in Friedreich's ataxia. *J Pediatr Orthop*, 4, 673–676

Cheung J, Halbertsma JPK, Veldhuizen AG, Sluiter WJ, Maurits NM, Cool JC & Van Horn JR. 2005. A preliminary study on electromyographic analysis of the paraspinal musculature in idiopathic scoliosis. *European Spine Journal*, 14(2), 130-137

Cheung J, Halbertsma JPK, Veldhuizen AG, Sluiter WJ, Maurits NM, Cool JC & Van Horn JR. 2004. The relation between electromyography and growth velocity of the spine in the evaluation of curve progression in idiopathic scoliosis. *Spine*, 29(9), 1011

Clague JE, Roberts N, Gibson H & Edwards RHT. 1995. Muscle imaging in health and disease. *Neuromuscular Disorders*, 5(3), 171-178

Coatney RW, 2001. Ultrasound imaging: principles and applications in rodent research. *Ilar Journal*, 42(3), 233-247

Daher YH, Lonstein JE, Winter RB & Bradford DS. 1985. Spinal deformities in patients with Friedreich's ataxia: a review of 19 patients. *J Pediatr Orthop* , 5, 553–557

Daube JR, 1991. AAEM minimonograph #11: Needle examination in clinical electromyography. *Muscle & nerve*, *14*(8), 685-700

Delatycki M & Corben L, 2012. Clinical Features of Friedreich Ataxia. *Journal of Child Neurology*, 27(9), 1133-1137

de Oliveira AS, Gianini PES, Camarini PMF & Bevilaqua-Grossi D. 2011. Electromyographic Analysis of Paravertebral Muscles in Patients with Idiopathic Scoliosis. *Spine*, 36(5), E334

Drake RL, Vogl W, Mitchell AWM & Gray H. 2005. Gray's Anatomy for Students. 2nd Edition. Philadelphia: Elsevier/Churchill Livingstone

Fidler MW & Jowett RL, 1976. Muscle imbalance in the aetiology of scoliosis. *Journal of Bone and Joint Surgery-British*, 58(2), 200

Florimond V, 2008. Basics of Surface Electromyography Applied to Psychophysiology. *Thought Technology Ltd*. Montreal, Canada

Ford DM, Bagnall KM, Clements CA & McFadden KD. 1987. Paraspinal muscle imbalance in adolescent idiopathic scoliosis. *Spine,* 9(4), 373

Frascarelli M, Rocchi L & Feola I. 1988. EMG computerized analysis of localized fatigue in Duchenne muscular dystrophy. *Muscle & nerve*, *11*(7), 757-761

Gardner-Medwin D, 1968. Studies of the carrier state in the Duchenne type of muscular dystrophy. 2. Quantitative electromyography as a method of carrier detection. *Journal of neurology, neurosurgery, and psychiatry*, *31*(2), 124

Gaudreault N, Arsenault AB, Larivière C, DeSerres SJ & Rivard CH. 2005. Assessment of the paraspinal muscles of subjects presenting an idiopathic scoliosis: an EMG pilot study. *BMC musculoskeletal disorders*, 6(1), 14

Geoffroy G, Barbeau A, Breton G , Lemieux B, Aube M, Leger C & Bouchard JP. 1976. Clinical description and roentgenologic evaluation of patients with Friedreich's ataxia. *Can J Neurol Sci*, 3, 279–286

Harding AE, 1981. Friedreich's ataxia: a clinical and genetic study of 90 families with an analysis of early diagnostic criteria and intrafamilial clustering of clinical features. *Brain*, 104, 589-620

Heckmatt JZ, Pier N & Dubowitz V. 1988. Real time ultrasound imaging of muscles. *Muscle & nerve*, 11(1), 56-65

Heckmatt J, Rodillo E, Doherty M, Willson K & Leeman S. 1989. Quantitative sonography of muscle. *Journal of child neurology*, *4*(1 suppl), S101-S106

Heckmatt JZ, Leeman S & Dubowitz V. 1982). Ultrasound imaging in the diagnosis of muscle disease. *The Journal of pediatrics*, *101*(5), 656-660

Hensinger RN & MacEwen GD, 1976 Spinal deformity in heritable neurological conditions: spinal muscular atrophy, Friedreich's ataxia, familial dysautonomia and Charcot-Marie-Tooth disease. *J Bone Joint Surg [Am]*, 58-A: 13–24

Herbison GJ, Jaweed MM & Ditunno JF, 1982. Muscle fiber types. *Archives of physical medicine and rehabilitation*, 63(5), 227

Hermens HJ, Stegman DF, Merletti R, Hagg G,Blok J, Rau G & Disselhorst-Klug C. 1999. SENIAM 8: European Recommendations for surface electromyography, *Roessingh Research and Development:* http://www.seniam.org/

Hete B & Shung KK, 1995. A study of the relationship between mechanical and ultrasonic properties of dystrophic and normal skeletal muscle. *Ultrasound in medicine & biology,* 21(3), 343-352

Hides J, Richardson C & Jull G. 1995. Magnetic resonance imaging and ultrasonography of the lumbar multifidus muscle comparison of two modalities. *Spine,* 20(1), 54-58

Hogrel JY, 2005. Clinical applications of surface electromyography in neuromuscular disorders. *Clinical Neurophysiology*, 35(2-3), 59-71

Hopf C, Scheidecker M, Steffan , Bodem F & Eysel P. 1998. Gait analysis in idiopathic scoliosis before and after surgery: a comparison of the pre- and postoperative muscle activation pattern. *European Spine Journal*, 7(1), 6-11

Hughes S, 2001. Medical ultrasound imaging. *Physics Education*, 36, 468

Jansen M, van Alfen N, Nijhuis van der Sanden MW, van Dijk JP, Pillen S & de Groot IJ. 2012. Quantitative muscle ultrasound is a promising longitudinal follow-up tool in Duchenne muscular dystrophy. *Neuromuscular Disorders*, *22*(4), 306-317

Kinali M, Manzur AY & Muntoni F. 2008. Recent developments in the management of Duchenne muscular dystrophy. *Paediatrics and Child Health*, 18(1), 22-26

Kennelly KP & Stokes MJ, 1993. Pattern of asymmetry of paraspinal muscle size in adolescent idiopathic scoliosis examined by real-time ultrasound imaging: a preliminary study. *Spine*, 18(7), 913

Kimura J, 1989. Electrodiagnosis in diseases of nerve and muscle. 2nd Edition. Philadelphia, FA Davis

Kossoff G, 2000. Basic physics and imaging characteristics of ultrasound. *World J Surg*, 24,134–142

Labelle H, Tohmé S, Duhaime M & Allard P. 1986. The natural history of scoliosis in Friedreich's ataxia. *J Bone Joint* Surg [Am], 68-A, 564–572

Lamminen AJAA, Jääskeläinen J, Rapola J & Suramo I. 1988. High-frequency ultrasonography of skeletal muscle in children with neuromuscular disease. *Journal of Ultrasound in Medicine*, *7*(9), 505-509

Lowery MM, Stoykov NS, Taflove A & Kuiken TA. 2002a. A Multi-layer finite element model of the surface EMG signal. *IEEE Trans BME,*49(5), 446-54

Machida M, 1999. Cause of idiopathic scoliosis. *Spine,* 24(24), 2576

Mannion AF, Meier M, Grob D & Müntener M. 1998. Paraspinal muscle fibre type alterations associated with scoliosis: an old problem revisited with new evidence. *European Spine Journal* ,7(4), 289-293

Maurits NM, Bollen AE, Windhausen A, De Jager AE &Van Der Hoeven JH. 2003. Muscle ultrasound analysis: normal values and differentiation between myopathies and neuropathies. *Ultrasound in medicine & biology*, 29(2), 215-225

McComas AJ, Sica REP & Currie S. 1971. An electrophysiological study of Duchenne dystrophy. *Journal of Neurology, Neurosurgery & Psychiatry*, 34(4), 461

Meier MP, Klein MP, Krebs D, Grob D & Müntener M. 1997. Fiber transformations in multifidus muscle of young patients with idiopathic scoliosis. *Spine*, 22(20), 2357

Merletti R & Parker P, 2005. Physiology, engineering, and noninvasive applications. *Electromyography*.

Milbrandt TA, Kunes JR & Karol LA. 2008. Friedreich's ataxia and scoliosis: the experience at two institutions. *J Pediatr Orthop,* 28(2), 234-8

Mooney V, Gulick J & Pozos R. 2000. A preliminary report on the effect of measured strength training in adolescent idiopathic scoliosis. *Journal of Spinal Disorders & Techniques*, 13(2), 102-107

Odermatt D, Mathieu PA, Beauséjour M, Aubin CÉ & Labelle H. 2003. Electromyographic study of adolescent idiopathic scoliosis patients treated with the Boston brace. J Orthop

Research. 21, 931-936

Pandolfo M, 2009. Friedreich ataxia: the clinical picture. *J Neurol,* 256, 3–8

Perdriolle R, Becchetti S, Vidal J & Lope zP. 1993. Mechanical process and growth. Essential factors in the progression of scoliosis. *Spine* 18, 343–349

Pillen S, Keimpema M, Nievelstein RAJ, Verrips A, Kruijsbergen-Raijmann W & Zwarts MJ. 2006. Skeletal muscle ultrasonography: visual versus quantitative evaluation. *Ultrasound in medicine & biology* 32(9), 1315-1321

Priez A, Duchene J & Goubel F, 1992. Duchenne muscular dystrophy quantification: a multivariate analysis of surface EMG. *Medical and Biological Engineering and Computing*, *30*(3), 283-291

Purnama IKE, Wilkinson MHF, Veldhuizen AG, van Ooijen PMA, Sardjono TA, Lubbers J & Verkerke GJ. 2009. Following Scoliosis Progression in the Spine using Ultrasound Imaging. *IFMBE Proceedings* 25, 600–602

Reuber M, Schultz A, McNeill T, Spencer D. 1983. Trunk muscle myoelectric activities in idiopathic scoliosis. *,* 8, 447–456

Riddle HF & Roaf R, 1955. Muscle imbalance in the causation of scoliosis. *Lancet* 268(6877): 1245

Ross E, MacGillivray TJ, Muir AY & Simpson A, 2009. Imaging of the musculoskeletal system using 3D ultrasound. J *Bone Joint Surg Br* 91-B, 451-452

Sahgal V, Shah A, Flanagan N, Schaffer M Kane W, Subramani V& Singh H. 1983. Morphologic and morphometric studies of muscle in idiopathic scoliosis. *Acta Orthopaedica*, 54(2), 242-251

Scholten RR, Pillen S, Verrips A & Zwarts MJ. 2003. Quantitative ultrasonography of skeletal muscles in children: normal values. *Muscle & nerve*, 27(6), 693-698

Sethi RKb & Thompson LL, 1989. The electromyographer's handbook. Second ed. Boston, Littele, Brown

Shapiro F& Specht L, 1993. The diagnosis and orthopaedic treatment of inherited muscular diseases of childhood. *J Bone Joint Surg Am*, 75(3), 439-54

Shimode M, Ryouji A & Kozo N. 2003. Asymmetry of Premotor Time in the Back Muscles of Adolescent Idiopathic Scoliosis. *Spine,* 28(22), 2535-2539

Sirca A & Kostevc V, 1985. The fibre type composition of thoracic and lumbar paravertebral muscles in man. *Journal of anatomy*, 141,131

Spencer GSG & Zorab PA, 1976. Spinal muscle in scoliosis: Part 1. Histology and histochemistry. *Journal of the Neurological Sciences,* 30(1), 137-142

Spencer GS & Eccles MJ , 1976. Spinal muscle in scoliosis. Part 2.The proportion and size of type 1 and type 2 skeletal muscle fibres measured using a computer-controlled microscope. *Journal of the Neurological Sciences*, 30,143–154

Stalberg E, Nandedkar S, Sanders DB, Falck B. 1996. Quantitative motor unit potential analysis. *J Clin Neurophysiol*, 13,401–422

Stegeman DF, Blok JH, Hermens HJ & Roeleveld K. 2000. Surface EMG models: properties and applications. *Journal of Electromyography and Kinesiology*, 10(5), 313-326

Stern LM & Clark BE, 1988. Investigation of scoliosis in Duchenne dystrophy using computerized tomography. *Muscle Nerve,* 11**,** 775-83

Thouin J F, 2005. Activité EMG des muscles du dos chez des patients dystrophiques. *Mémoire de Maîtrise*, Université de Montréal

Treece G, Prager R, Gee A & Berman L. 2001. 3D ultrasound measurement of large organ volume. *Medical Image Analysis*, 5(1), 41-54

Tsirikos A & Smith I, 2012. Scoliosis in patients with Friedreich's ataxia. *J Bone Joint Surg Br*, 94-B, 684–9

Türker KS, 1993. Electromyography: some methodological problems and issues. *Physical therapy,* 73(10), 698

Valentino B, Maccauro L, Mango G, Melito F & Fabozzo A. 1985. Electromyography for the investigation and early diagnosis of scoliosis. *Surgical and Radiologic Anatomy,* 7(1), 55-59

Van den Bosch J, 1963. Investigations of the carrier state in the Duchenne type dystrophy. *In Research in Muscular Dystrophy: Proceedings of the Second Symposium, edited by the Research Committee of the Muscular Dystrophy Group of Great Britain,* Montreal, JB Lippincott

Wattjes MP, Kley RA & Fischer D. 2010. Neuromuscular imaging in inherited muscle diseases. *European radiology*, *20*(10), 2447-2460

Weiss HR, 1993. Imbalance of electromyographic activity and physical rehabilitation of patients with idiopathic scoliosis. *European Spine Journal*, 1(4), 240-243

Whittaker JL, Teyhen DS, Elliott JM, Cook K, Langevin HM, Dahl HH & Stokes M. 2007. Rehabilitative ultrasound imaging: understanding the technology and its applications. *Journal of Orthopaedic and Sports Physical Therapy*, 37(8), 434

Wood S, 1996. Magnetic resonance imaging investigation of trunk muscle asymmetry in adolescent idiopathic scoliosis. M. Sc, Thesis, Queen's University, Kingston, ON

Zaidman CM, Connolly AM, Malkus EC, Florence JM & Pestronk A. 2010. Quantitative ultrasound using backscatter analysis in Duchenne and Becker muscular dystrophy. *Neuromuscular Disorders*, *20*(12), 805-809

Zetterberg C, Björk R, Örtengren R & Andersson GBJ, 1984. Electromyography of the paravertebral muscles in idiopathic scoliosis: measurements of amplitude and spectral changes under load. *Acta Orthopaedica*, 55(3), 304-309

Zoabli G, Mathieu PA & Aubin CE. 2008. Magnetic resonance imaging of the erector spinae muscles in Duchenne muscular dystrophy: implication for scoliotic deformities. *Scoliosis,* 3, 21

Zoabli G, Mathieu PA & Aubin CÉ. 2007. Back muscles biometry in adolescent idiopathic scoliosis. *The Spine Journal*, *7*(3), 338-344

Zsidai A, 2001. Ultrasound based spinal column examination systems. *Series Physical Eduation and Sport*, 1(8), 1-12

Zuberi SM, Matta N, Nawaz S, Stephenson JB, McWilliam RC & Hollman A. 1999. Muscle ultrasound in the assessment of suspected neuromuscular disease in childhood. *Neuromuscular Disorders,* 9(4), 203-207

Zuk T, 1962. The role of spinal and abdominal muscles in the pathogenesis of scoliosis. *Journal of Bone and Joint Surgery-British*, 44(1), 102

Appendix A

Sainte-Justine Ethical Comitte Approval

Monsieur Pierre A. Mathieu
Institut de génie biomédical
C.P. 6128, succ. Centre-ville
Montréal Québec H3C 3J7

CHU Sainte-Justine
Le centre hospitalier universitaire mère-enfant

Pour l'amour des enfants

Université de Montréal

OBJET: Titre du projet: Phase 2: Activité EMG et imagerie des muscles du dos de patients atteints de DMD et AF

No. de dossier: 3332

Responsables du projet: Pierre A. Mathieu Ph. D., chercheur responsable au CHU Sainte-Justine. Chercheur principal: Fawzieh Sleem. Collaborateurs: Farida Chériet, Carl-Éric Aubin, Julie Joncas et Christian Bellefleur

Monsieur,

Votre demande d'amendement a été approuvée par notre comité en date du 9 mai 2013. L'amendement porte sur la modification de la compensation et la modification du titre du Projet.

Veuillez trouver ci-joint la liste des documents approuvés ainsi que vos formulaires d'information et de consentement estampillés dont nous prions de vous servir d'une copie pour distribution.

Nous vous souhaitons bonne chance dans la continuité de votre projet et vous prions de recevoir nos meilleures salutations.

Geneviève Cardinal, juriste
Vice-Présidente du Comité d'éthique de la recherche

GC/mhl

CHU Sainte-Justine
Le centre hospitalier universitaire mère-enfant
Pour l'amour des enfants

Université de Montréal

[AF: CONSENTEMENT PATIENT]

1. Titre du projet de recherche

Phase 2: Activité EMG et imagerie des muscles du dos des patients atteints de DMD et AF

2. Nom des chercheurs

Pierre A Mathieu, Ph.D. Centre de recherche, CHU Sainte-Justine.
Fawzieh Sleem, étudiante à la maîtrise, Centre de recherche, CHU Sainte-Justine.

Source de financement

Conseil de recherches en science naturelles et en génie (CRSNG)

3. Invitation à participer à un projet de recherche

Le département d'orthopédie de l'CHU Sainte-Justine participe à des recherches dans le but d'améliorer les traitements chez les enfants souffrant de l'Ataxie de Friedreich (AF). Nous sollicitons aujourd'hui la participation de votre enfant. Nous vous invitons à lire ce formulaire d'information afin de décider si vous êtes intéressé à ce que votre enfant participe à ce projet de recherche. Il est important de bien comprendre ce formulaire. Pour ce faire poser toutes les questions qui vous viennent à l'esprit. De plus, prenez le temps nécessaire pour prendre votre décision.

4. Nature et objectif de cette recherche

Votre enfant souffre de l'Ataxie de Friedreich. Cette condition peut causer, entre autres, une déformation de la colonne vertébrale que l'on nomme scoliose.

L'objectif principal de cette recherche est de mieux comprendre le rôle des muscles du dos dans le développement de la scoliose en vue de la prévenir si possible et d'en ralentir le développement.

5. Comment se déroulera le projet ?

Si vous choisissez de prendre part de l'étude, nous demandons à votre enfant sa participation à ce projet à deux reprises à l'intérieur de 12 mois environ. Ceci se déroulera à l'CHU Sainte-Justine. La première visite aura lieu lorsque vous vous présentez avec votre enfant à un laboratoire d'étude du mouvement pour réaliser le protocole expérimentale.

Le personnel de recherche mesurera la taille, le poids ainsi que la hauteur des épaules et la façon dont le corps de votre enfant se penche vers l'avant et vers le cote en position assise. La prise de ces mesures devrait prendre au maximum 15 minutes.

Ensuite on appliquera une crème sur la peau du dos et du ventre, et collera des petits capteurs qui serviront à mesurer l'activité électrique des muscles de votre enfant ce qui consiste a des mesures avec l'électromyogramme (EMG). Cela ne causera pas de douleur. Votre enfant demeurera assis pendant toute cette partie du protocole. Nous installerons ensuite un harnais

autour de ses épaules et nous demanderons a votre enfant de forcer avec les muscles du tronc afin de garder une position droite malgré l`application décharges qui tenteront de la déstabiliser.

Puisque les charges utilisées sont petites, votre enfant ne devrait pas éprouver de courbatures suite au protocole. La prise de ces mesures de l`activité musculaire devrait prendre au maximum 45 minutes. Suivra l`échographie des muscles de dos dans le même laboratoire. Pour la prise des images, on demandera à votre enfant de se coucher sur une table les bras placés le long du corps. Pour son confort et pour maintenir l'alignement de la colonne vertébrale, des serviettes roulées sous le front et les épaules seront utilisées. Un oreiller sera placé sous les hanches pour éliminer la lordose lombaire. Une crème échographique sera appliquée le long de la colonne vertébrale pour assurer le contact avec le transducteur échographique qui sera déplacé de part et d'autre de la colonne pour acquérir les images des muscles du dos.

6. Quels sont les avantages et bénéfices ?

La participation de votre enfant permettra d'améliorer les connaissances et peut-être éventuellement le traitement de patients atteints de l'Ataxie de Friedreich.

7. Quels sont les inconvénients et les risques ?

L`électromyogramme (EMG) et l`échographie sont sans danger. Ces examens sont non invasifs car aucun rayonnement ionisant n'est impliqué et sont sans douleur car seul un contact avec la peau avec des matériaux inertes est effectué. Le seul inconvénient réel pour les sujets recrutés est le temps requis passé en laboratoire qui est de 2 heures quarante-cinq minutes.

8. Y a-t-il d`autres options possible ?

Vous pouvez refuser que votre enfant participe au projet de recherche et cela n`interféra pas avec les traitements que votre médecin pourra lui offrir.

9. Dans quel cas l`étude peut-elle être suspendue ?

Si votre enfant présente un malaise lors de son passage au laboratoire, les tests seront immédiatement suspendus et de l'aide médical sera demandée. Dans la phase I de ce projet impliquant 10 patients, un tel événement ne s'est jamais produit.

10. Comment la confidentialité est-elle assurée ?

Tous les renseignements que nous obtiendrons seront gardés confidentiellement à moins d`une autorisation de votre part ou d`une exception de la loi. Ainsi, ces renseignements seront codés avec un numéro attribué au hasard, et mis sous clé dans nos locaux au Centre de recherche de l`CHU Sainte-Justine sous la responsabilité de Prof. Pierre A. Mathieu.

La durée de conservation des données est de 7 ans.

Cependant, à des fins de vérification, il est possible qu`un délégué du Comité d`Éthique de l'CHU Sainte-Justine, ou de l'organisme subventionnaire (CRSNG) consultent nos données de recherche et le dossier médical de votre enfant.

Par ailleurs, les résultats de cette recherche pourront communiqués dans des congrès scientifiques ou publiés dans des journaux scientifiques mais aucune information pouvant conduire à l'identification de votre enfant ne sera dévoilée.

À des fins de protection, le Ministère de la santé et des services sociaux pourrait avoir accès à votre nom et prénom ainsi que ceux de votre enfant, ses coordonnées (adresse et numéro de téléphone), la date de début et de fin de sa participation au projet jusqu'à un an après la fin de projet.

11. Responsabilité des chercheurs

En signant ce formulaire de consentement, vous ne renoncez a aucun de vos droits prévus par la loi ni à ceux de votre enfant. De plus, vous ne libérez pas les investigateurs et le promoteur de leur responsabilité légale et professionnelle.

12. Compensation prévue pour vos dépenses et inconvénients

Une compensation de 125 dollars est prévue pour la totalité du protocole de recherche.

13. Commercialisation

Non applicable dans ce projet.

14. Conflits d'intérêts

Il n`y a aucun conflit d`intérêt car les chercheurs ne sont ni actionnaires ni payés par une compagnie quelconque pour réaliser cette étude.

15. Liberté de participation

La participation de votre enfant à ce projet de recherche est libre et volontaire. Toute nouvelle connaissance susceptible de remettre en question la décision que votre enfant de participer à la recherche vous sera communiquée. Vous pouvez retirer votre enfant de cette recherche en tout temps et les données non analysées seront détruits.

16. En cas de questions ou de difficultés, avec qui peut-on communiquer ?

Pour plus d'information concernant cette recherche, contactez le chercheur responsable de cette recherche au CHU Sainte –Justine, Pierre A. Mathieu au (514) 343-6369. Pour tout renseignement sur les droits de votre enfant à titre de participant à ce projet de recherche, vous pouvez contactez le commissaire local aux plaintes et à la qualité des services de l'CHU Sainte-Justine au (514) 345-4749.

CHU Sainte-Justine
Le centre hospitalier universitaire mère-enfant
Pour l'amour des enfants
Université de Montréal

[AF: CONSENTEMENT PATIENT]

17. Consentement et assentiment

On m'a expliqué la nature et le déroulement du projet de recherche. J'ai pris connaissance du formulaire de consentement et on m'en a remis un exemplaire. J'ai eu l'occasion de poser des questions auxquelles on a répondu à ma satisfaction. Après réflexion, j'accepte de participer (18 ans et plus) ou que mon enfant participe à ce projet de recherche. J'autorise l'équipe de recherche à consulter le dossier médical (18 ans et plus) ou celui de mon enfant pour obtenir les informations pertinentes à ce projet.

Nom de l'enfant (lettres moulées)	(signature) (si l'enfant est capable de comprendre la nature du projet)	Date

Assentiment verbal de l'enfant incapable de signer mais capable de comprendre la nature de ce projet: oui___ non___

Nom du parent, tuteur ou du participant de 18 ans et plus (lettres moulées)	Consentement (signature)	Date

J'ai expliqué au participant et/ou à son parent/tuteur tous les aspects pertinents de la recherche et j'ai répondu aux questions qu'ils m'ont posées. Je leur ai indiqué que la participation au projet de recherche est libre et volontaire et que la participation peut être cessée en tout temps.

Nom de la personne qui a obtenu la signature de consentement (lettres moulées)	Date

Appendix B

The StradWin Calibration Procedure

(From: http://mi.eng.cam.ac.uk/~rwp/stradwin/docs/calibrate.htm)

The required depth setting and point of focus for the US probe must be first set on the US machine before initiating the live image display within StradWin which permits on-line viewing of the US images alongside a window where the position of the US probe within the measurement volume is displayed during the image acquisition. The outline of the measurement volume changes colour dependent on the state of the tracking tool fixed on the US probe. If it is green the tool is within the volume, if it is yellow the tracking tool is approaching the edge of the volume and if it is red it is outside the volume or the line-of-sight between the tool and position sensor unit has been blocked. A sample of such images is shown in the following picture.

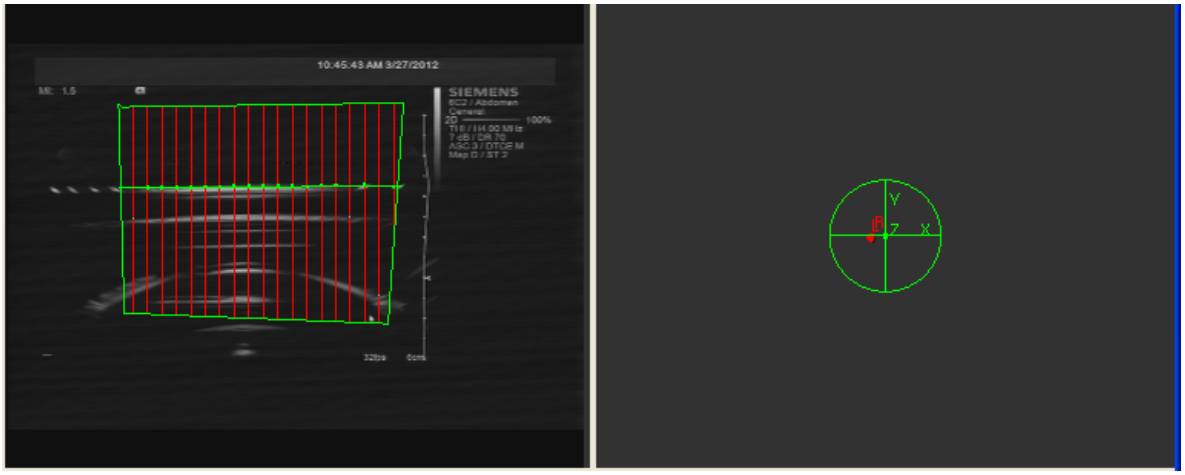

Figure A: StradWin screenshot in real time. On the left, this is the US image generated from the Acuson and on the right, the circle show the status of the position sensor: a green circle indicate that sensor on the US probe is detected by the Polaris camera and the red spot indicate the position of the US probe.

With both available US images and position tracking, the **Record** task page should be selected. Both the image source and position source configuration details have to be

checked to ensure they are correct for the US probe, depth and point of focus settings being used. Most of the image source configuration settings remain as default; the source of the image data should have been automatically detected. The auto image cropping function will set the height, width and offsets for the US image being recorded or they can be set manually.

Finally, the number of focal points and the position of the first focal point for the US beam must be selected. Position source configuration should automatically be detected when StradWin starts, however, if this has not happened details can be selected in the position source configuration menu. On the **Record** task page the frame acquisition rate should be set to full speed and the image format should be set to Greyscale. Finally, the data format must be selected, B-scan.

Calibration is initiated on the **Probe Calib** task page. The first part of the calibration process is the **temporal calibration** which is carried out by holding the US probe steady in a water bath near to and perpendicular to its bottom. The probe is then moved swiftly upwards to induce a significant change in both the image content and the position reading measurement. As shown below, the change in position of the line showing the bottom of the water bath and the change in the position reading for the probe are used to calculate the temporal offset between the images and positions. This process should be repeated 5 times to give an averaged calibration result.

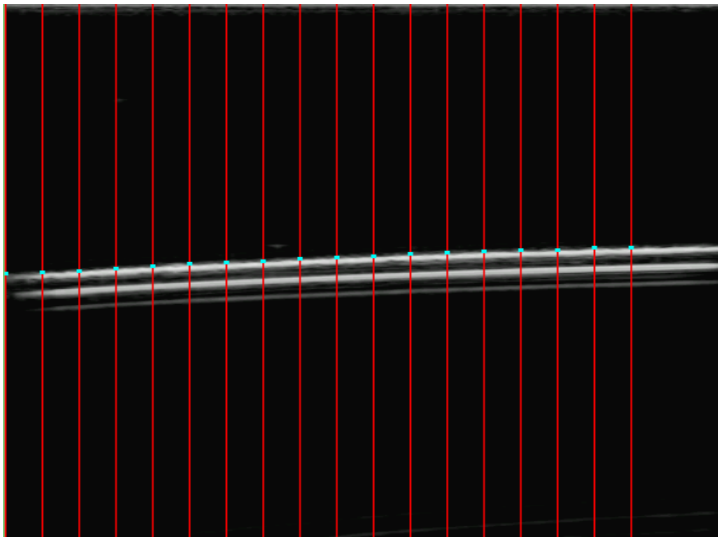

Figure B : StradWin screenshot in real time. The position of the line showing the bottom of the water bath and the change in the position reading for the probe used to calculate the temporal offset between the images and positions.

The next stage for calibration is the **spatial calibration** which requires a simple flat surface phantom immersed within the water bath. In this stage the user requires to input the temperature of the water in the water bath. Room temperature water should be used for calibration as this avoids any change in temperature during the process which will affect the result. However, a new algorithm has been incorporated into StradWin which compensates for the effects of using lower temperature water during calibration. Final adjustments should now be made to the US image using the Tx (Transmit gain), Rx (Received gain) and the TGC (Time Gain Compensation) controls on the US machine. The appearance of the surface of the single walled phantom, which appears as a line on the B-scan images, should be set so that it is barely visible. This helps to remove repeated surface artefacts from the image and aids the line detection process.

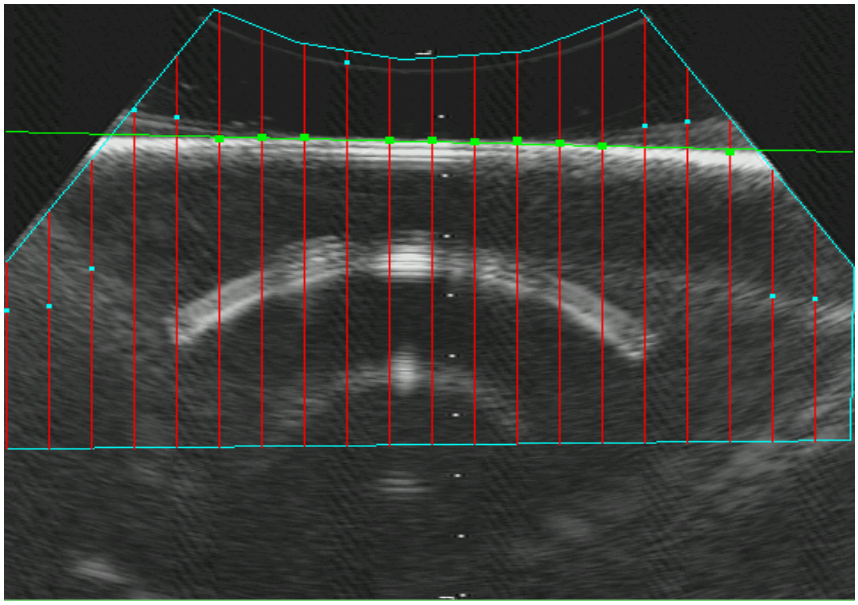

Figure C: The appearance of the surface of the single walled phantom on StradWin screenshot in real time

The dimensions of the pixels which make up the US image must be determined by measuring the width and height of the image. A good image of the bottom of the water bath should be obtained and then frozen using the US machine controls this will causes the image on StradWin to also freeze. The measurement callipers on the US machine are used to determine the width of the image. Keeping the image frozen the image width must be measured across the same point in StradWin using a further set of callipers. A set slider control is used to set the width of the line in StradWin using the measurement obtained from the US machine callipers. This process is repeated to measure height on the US image before the image display is unfrozen. This procedure is slightly different for curvilinear probes.

A set of calibration movements have been devised to ensure a sufficient range of motion of the probe is sampled for accurate calibration. The probe should be moved through the pre-defined set of motions shown in figure A.

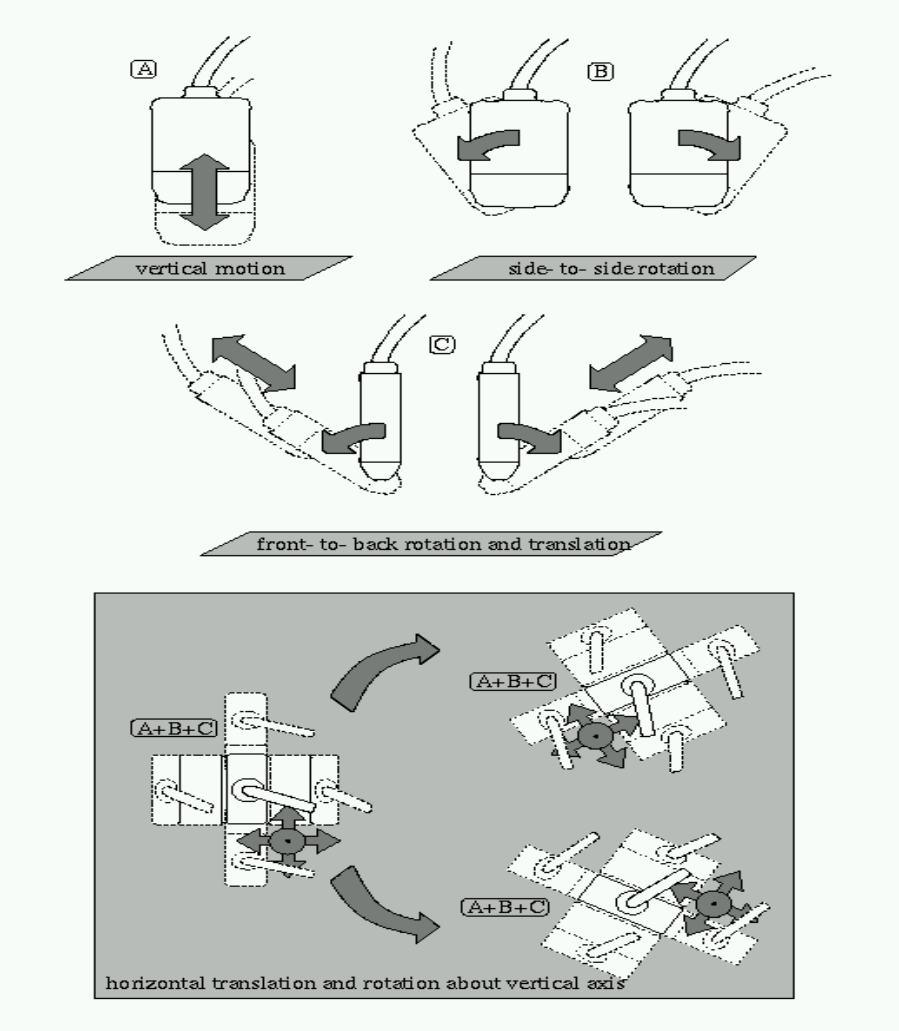

Figure D: Probe movements carried out during spatial calibration. This is necessary to define both the spatial calibration parameters and the location of the calibration plane (Treece et al. 2003).

When the probe is moved into one of the calibration positions, a good image of the bottom of the water bath should be obtained and the line detector shown on the *S*tradWin live image should be checked to ensure it is correctly locked on to the line before the image is accepted for use in calibration. If the line detector is having difficulty locking onto the line a message stating 'No valid Line' will be shown. At least 40 lines should be captured using the full range or probe positions in order to give a reliable calibration. Once a set of lines has been collected, click the 'Solve for Spatial calibration' button to run the calibration algorithm. This algorithm uses the position information extracted from the lines to

determine the coordinate transforms between the US probe, tracking system and the real world system. A good calibration should return an RMS error of less than 0.2 cm. Details of the depth setting and probe frequency need to be input before the calibration is accepted for scanning. At this point the calibration can be saved as a template to be reloaded for use at any future date. Before saving the calibration as a template ensure that the desired frame rate data format are selected on the **Record** task page.